HR Wallingford
Working with water

Methods for predicting suspensions of mud

TR104 R2

October 2012

Document information

Report title	Methods for predicting suspensions of mud
Client	HR Wallingford Company Research
Client Representative	Mr I H Townend
Project No.	DDY0409
Report No.	TR104
Project Manager	Dr A J Manning
Project Director	Dr R J S Whitehouse

Document history

Date	Release	Prepared	Approved	Authorised	Notes
May 2000	1.0	RLS		RJSW	Supporting document for derivations of formulae in 'Dynamics of Estuarine Muds'.
17/10/12	2.0	RLS	AJM	RJSW	Elaborates the derivations and adds appendix describing results of Company Research Project on settling velocity of mud flocs.

Prepared R L Soulsby

Approved A J Manning

Authorised R Whitehouse

Summary

Methods for predicting suspensions of mud

Report TR104
October 2012

This report elaborates and updates the supporting information on unpublished methods quoted in the book ‘Dynamics of Estuarine Muds’ (Whitehouse *et al*., 2000), which were described in Release 1.0 of the report. They include prediction methods for: bed shear-stresses on smooth (muddy) beds, (hindered) settling velocity of flocculated mud suspensions, and the concentration profile of suspended mud. Release 2.0 also includes an appendix describing a new method for predicting (unhindered) settling velocity and mass settling flux of flocculated mud suspensions developed in a recent company research project.

Contents

1 Introduction

This report was written initially in 2000 as supporting information for the book 'Dynamics of Estuarine Muds' (Whitehouse *et al.*, 2000), referred to subsequently as DEM. It elaborated the derivations, developed by the present author, of unpublished methods quoted in the book that relate to bed shear-stresses on smooth (muddy) beds, (hindered) settling velocity of flocculated mud suspensions, and the concentration profile of suspended mud. Release 2.0 (2012) adds extra detail to these derivations, and presents as an appendix a new method of predicting (unhindered) settling velocity and mass settling flux developed in a recent company research project, that makes use of a large field data-set collected by Dr Andy Manning. The appendix is equivalent to HR Wallingford Technical Note DDY0409-01 (Soulsby and Manning, 2012).

2 Bed shear-stresses

This section is an updated version of Section 3.4 of DEM, together with a more recent method.

2.1 METHOD PRESENTED IN 'DYNAMICS OF ESTUARINE MUDS'

The main hydrodynamic parameter that controls the erosion, suspension and deposition of muds is the *bed shear-stress*, which is the frictional force exerted by the flow per unit area of bed. Methods of calculating the bed shear-stress produced by currents (τ_c) and waves (τ_w), separately or in combination, are therefore needed. The methods are broadly similar to those used for beds of coarser sediments, but with the difference that the flow is usually assumed to be hydrodynamically smooth for muds whereas it is usually treated as hydrodynamically rough for sands and gravels. The formulae described below are adaptations to the case of hydrodynamically smooth flow of those presented in Soulsby (1997).

Note, however, that in certain cases a mud bed may be very rough as a result of trawling activities or bioturbation; for example, box cores of muddy sediments taken at depths of up to 60 m in the Clyde Sea, western Scotland, were found to have a very disturbed irregular surface with lumps of firm mud several centimetres in height. Bed roughnesses in estuaries may also sometimes be large, for example in areas with a network of fine drainage channels. In these cases the *total* bed shear-stress will be governed by the large roughness which incorporates the form-drag created by the pressure field around the roughness elements. Nevertheless, the erosion and deposition of the mud will depend more on the smooth flow over the intervening areas, and the smooth-hydrodynamic equations given below can be used.

In many cases both currents and waves make significant contributions to the bed shear-stress. The resulting bed shear-stress consists of a steady component due to the current together with an oscillatory component due to the waves. If the current and wave velocities over a smooth bed are sufficiently small that the flow remains laminar, then the combined bed shear-stresses are simply a linear addition of the laminar current-alone and wave-alone shear-stresses. However, in stronger currents and waves the flow will be turbulent, and the turbulence generated in the current and wave boundary layers then adds in a non-linear fashion. Because of this, the mean and oscillatory components of the stress are enhanced beyond the values which would result from a simple linear addition of the wave-alone and current-alone stresses.

The bed shear-stress $\tau(t)$ varies through a wave cycle, with the most important quantities for use in sediment calculations being:

- the mean value, τ_m, over the wave-cycle,
- the maximum value, τ_{max}, during the wave-cycle,
- the root-mean-square value, τ_{rms}, taken over the wave-cycle.

The mean, τ_m, is used for determining the friction governing the current, and for determining diffusion of sediment into the outer flow; the maximum, τ_{max}, is used to determine the threshold of sediment motion, and diffusion very near the bed; and τ_{rms} is a good average measure of the shear-stress, particularly useful in random waves.

More than twenty different theories and models have been proposed to describe this process, but almost all of them have concentrated on the case of a rough turbulent flow, as would be found over a coarse sand or gravel bed, rather than the smooth turbulent flow commonly found over a mud bed. Some of these theories were discussed and intercompared by Soulsby *et al.* (1993). A parametric fitting method for some of the theories was presented by Soulsby (1997) in terms of the nondimensional quantity $X = \tau_c/(\tau_c + \tau_w)$.

The different theories differ markedly in their predictions, and in the goodness of their fit to data (Soulsby *et al*., 1993). The best performing analytical theories were those of Fredsøe (1984) and Grant and Madsen (1979), although both are complicated to use. In view of this, the following equation, which has the same general form as that fitted to the theories, was proposed by Soulsby (1995) as a direct fit to 61 laboratory measurements and 70 field measurements of the cycle-mean bed shear-stress τ_m (all for rough beds):

$$\tau_m = \tau_c\left[1 + 1.2\left(\frac{\tau_w}{\tau_c + \tau_w}\right)^{3.2}\right] \qquad (1)$$

in which τ_c and τ_w are the bed shear-stresses which would occur due to the current alone and to the wave alone, respectively.

The corresponding expression for τ_{max} is given by a vector addition of τ_m from Equation (1) and τ_w:

$$\tau_{max} = \left[\left(\tau_m + \tau_w\left|\cos\phi\right|\right)^2 + \left(\tau_w\left|\sin\phi\right|\right)^2\right]^{1/2} \qquad (2)$$

where ϕ = angle between current direction and direction of wave travel.

This is based on an assumption that the enhancement of the oscillatory component of stress caused by the current-induced turbulence is negligible (but note that many of the more sophisticated theories do account for this). Similarly, the root-mean-square bed shear-stress is given by:

$$\tau_{rms} = \left(\tau_m{}^2 + \frac{1}{2}\tau_w{}^2\right)^{1/2} \qquad (3)$$

As indicated, the various theories and Equation (1) were all designed for rough-bed conditions. A comprehensive set of laboratory measurements made by Arnskov *et al*. (1993) of bed shear-stress generated by combined waves and currents over a smooth solid bed gives some indication of the flow behaviour over smooth mud beds (Figure 1). They found a significant non-linear enhancement of τ_m for wave-dominated conditions, but no enhancement for current-dominated conditions. Their measurements showed little or no enhancement of τ_{max}, contrary to the predictions of most rough-bed theoretical models. They also found evidence that current-generated turbulence was suppressed by large waves. They tested the rough-bed theoretical model of Fredsøe (1984) against this set of smooth-bed data and found it gave poor agreement. Equation (1) also gives a poor fit to these data.

Although the general formulation used to derive Equation (1) was based on data for rough beds, it seems reasonable to extend the basic nonlinearity it expresses to the case of smooth beds by fitting its two free coefficients (set as 1. 2 and 3.2 in Equation 1) to the data of Arnskov *et al*. (1993). Least squares fitting of Equation (1) to the Arnskov data gives coefficient values of 9 and 9. The fitted equation for the mean bed shear-stress generated by a current and waves over a smooth bed is thus:

$$\tau_m = \tau_c \left[1 + 9 \left(\frac{\tau_w}{\tau_c + \tau_w} \right)^9 \right] \tag{4}$$

The values of τ_c and τ_w are calculated using the smooth-turbulent methods given in Sections 3.2 and 3.3 of DEM. The calculations of τ_{max} and τ_{rms} are given by Equations (2) and (3).

Figure 1 shows that Equations (4) and (2) give a reasonably good fit to the smooth-bed measurements of τ_m and τ_{max} made by Arnskov *et al.* (1993) and Sleath (1990) for waves travelling at 90° to a current. The shear-stresses are plotted in terms of nondimensional parameters X, Y and Z, as defined on the figure. Similar agreement was found for angles of 72° and 108°.

2.2 METHOD OF SOULSBY AND CLARKE (2005)

Since publication of 'Dynamics of Estuarine Muds', further research in the ESTPROC project led to a new and more general method of predicting bed shear-stresses due to currents and waves, separately or in combination, over both smooth and rough beds (Soulsby and Clarke, 2005). This method is now preferred to that given by Equation (4), as it is more general. In addition, the experiments by Arnskov *et al.* (1993) were at small scale, and the large values of Y observed for small values of X are now believed to be probably due to re-laminarisation of the flow. Soulsby and Clarke (2005) therefore paid greater attention to a larger scale data-set by Lodahl *et al.* (1998), and obtained good agreement, whereas their method under-estimated the mean bed shear-stresses of the Arnskov data by about a factor of two, for the reason stated. An extension of the *rough*-turbulent version of the Soulsby and Clarke (2005) method was made by Malarkey and Davies (2012).

3 *Settling velocity*

This section elaborates the derivation of a formula for the settling velocity of mud flocs, including the hindering effects encountered at large concentrations, which was summarised in DEM, pp. 89 - 92. It also presents an alternative approach for non-hindered settling velocity developed in a recent Company Research project (detailed in Appendix A), and some notes on experience of implementing the new method in a TELEMAC3D model.

3.1 DERIVATION OF HINDERED SETTLING FORMULA PRESENTED IN 'DYNAMICS OF ESTUARINE MUDS'

It is first necessary to distinguish various measures of density and concentration:

- the water-density ρ,
- the sediment grain density ρ_s,
- the effective density of the flocs including trapped water ρ_e,

- the mass (or dry) concentration of the suspension C_M,
- the volume concentration of grains in the suspension C,
- the volume concentration of flocs in the suspension C_f,
- and the volume concentration of sediment grains inside the floc C_{in}.

The first four have units of density (kg.m^{-3}) and the last three are dimensionless. They can be inter-related as follows:

$$C_M = \rho_s C$$

$$C = C_f C_{in}$$

$$C_f = \frac{(\rho_s - \rho)C}{(\rho_e - \rho)}$$

$$\rho_e = \rho + C_{in}(\rho_s - \rho)$$

The median settling velocity w_{50} of cohesive sediment is strongly dependent on the suspended sediment concentration. For lowish concentrations, w_{50} increases with increasing suspended sediment concentration C_M. The relationship may be approximated by the following empirical form of equation which is valid for dry mass concentrations up to a limit in the range 2 to 4 kg.m^{-3}.

$$w_{50} = kC_M{}^m \qquad (5)$$

where k and m are coefficients with appropriate dimensions, whose values vary considerably for different estuaries. For example, values of k and m displayed in Figure 20 of DEM vary in the approximate ranges k = 0.0002 to 0.002 and m = 0.6 to 1.4 in SI units (w_{50} in m.s^{-1} and C_M in kg.m^{-3}).

Hindered settling is the process by which a high concentration of settling flocs interferes with the surrounding flow of fluid. It usually commences at a suspended sediment concentration of between 2 kg.m^{-3} and 10 kg.m^{-3} (Krone, 1972; Burt and Stevenson, 1983; Puls and Kuehl, 1986). The settling velocity increases for larger concentrations at a slower rate than given by Equation (5) up to a peak and eventually decreases rapidly at very high concentrations. An example of settling velocity data for the Severn Estuary is given in Figure 2.

An approach which covers both low and high concentrations of flocculated mud can be derived from the Soulsby (1997, Equation 103) formula for the settling velocity w_{sC} of both low and high concentrations of sand:

$$W_s C = \frac{\nu}{d_s}\left\{\left[10.36^2 + 1.049(1 - C_s)^{4.7} D_{*s}{}^3\right]^{1/2} - 10.36\right\} \qquad (6)$$

where ν = kinematic viscosity of water
d_s = sand grain diameter
D_{*s} = dimensionless sand grain diameter
C_s = volume-concentration of sand.

We draw an analogy between the solid, high-density grains of sand, of diameter d_s and density ρ_s, and the loose, low-density assemblages of clay and silt that comprise flocs. Accordingly we replace d_s with the effective floc diameter d_e, and replace density ρ_s of sand grains with the effective density ρ_e of the flocs. The effective floc diameter is the diameter of a sphere of the same volume, and the effective density includes the mass of the water trapped within the floc as well as that of the sediment grains within it. The volume concentration of sand grains, C_s, is replaced with the volume concentration of flocs, C_f (i.e. the proportion of a unit volume of suspension that is occupied by flocs). This is because the hindered settling effect depends on the size of the gaps between the flocs being comparable with their diameter, so that volume-concentration rather than mass-concentration is the relevant factor. With this analogy, Equation (6) becomes for flocs:

$$w_{50}=\frac{v}{d_e}\left\{\left[10.36^2+1.049\left(1-C_f\right)^{4.7}D_{*f}^{\,3}\right]^{1/2}-10.36\right\} \tag{7}$$

and $D_{*f}=d_e\left[\frac{g(\rho_e-\rho)}{\rho v^2}\right]^{1/3}$ is the dimensionless floc diameter. (8)

At low concentrations (C_f << 1), we seek a relationship between d_e and other variables that makes the reduced version of Equation (7) compatible with the observed dependence of settling velocity on concentration given by Equation (5). If, in addition, the term $(1.049/10.36^2)D_{*f}^{\,3}$ is << 1, then expansion of the square root in Equation (7) and use of Equation (8) leads to the approximate expression:

$$w_{50}\approx\frac{1.049g(\rho_e-\rho)d_e^2}{2\times10.36\rho\nu} \tag{9}$$

For consistency between the theoretical and empirical expressions, we equate Equation (9) with Equation (5) written in the form $w_{50}=k\rho_s^{\,m}C^m$ to yield an expression for the effective floc diameter d_e which varies with the volume concentration C of the suspension according to the relationship

$$d_e=\ell C^{\frac{m}{2}} \tag{10}$$

where ℓ is a length-scale, and m is the power coefficient in Equation (5). Comparing Eqs (9) and (10), the length-scale ℓ must be given by the relationship

$$\ell=\left[\frac{19.8\rho\nu\rho_s^m k}{g(\rho_e-\rho)}\right]^{1/2} \tag{11}$$

Equation (7) is equivalent to Equation (5) at low concentrations, but at higher concentrations a maximum settling velocity is found beyond which w_{50} rapidly decreases with C_M. The coefficients k, m and C_{in} can be obtained by calibration against measured settling velocity curves. Values of C_{in}, the internal floc concentrations, are found to range from about 0.025 to 0.04, with C_{in} = 0.03 as a default value. These values compare with direct estimates of C_{in} from settling velocity data which show a wider range of values between 0.006 and 0.123 (Fennessy *et al*., 1994). Comparisons of Equation (7) [Equation (5.12) in DEM] against data from the Severn Estuary, using optimised values of the coefficients k = 0.00043 (S.I. units), m = 1.06, C_f = 0.032 are shown in Figure 2.

3.2 CRITERION FOR IMPORTANCE OF HINDERING

The criterion for deciding whether hindering has an important effect is usually quoted in terms of a limiting mass concentration. However, in different parts of this report a variety of limiting concentrations (or ranges of values) are quoted, drawn from various sources in the literature: 2 to 4 $kg.m^{-3}$, 2 to 10 $kg.m^{-3}$, and 3 $kg.m^{-3}$. We can use Equation (7) to quantify this criterion, which depends on the variables k, m and C_f, as well as the stringency of what is regarded as a significant effect. We input into Equation (7) values of k and m (all in S.I. units) for: the Parrett Estuary (k, m) = (0.0003, 0.69), the Thames Estuary (0.0017, 1.37), and commonly-used default values (0.001, 1.0), together with values of C_f in the range 0.025 to 0.04. These values embrace all the estuaries shown in Fig. 20 of DEM. The outputs from Equation (7) are compared with the unhindered settling velocities given by Equation (5). We find that the limiting mass concentration for which Equation (7) deviates by more than 10 per cent from the simple power law Equation (5) is in the range 1.1 to 2.4 $kg.m^{-3}$ (depending on k, m and C_f). Similarly, a deviation of more than 20 per cent occurs for a limiting mass concentration in the range 2.2 to 4.9 $kg.m^{-3}$. It thus seems that the various limiting concentrations quoted in this report correspond roughly to a 20 per cent reduction in settling velocity due to hindering effects. However, if 10 per cent accuracy is required, then hindering effects should be included for all concentrations in excess of 1 $kg.m^{-3}$.

3.3 SETTLING VELOCITY FORMULATION INCLUDING DEPENDENCE ON SHEAR-STRESS

An alternative approach to the prediction of the settling velocity of suspended flocculated mud was developed in HR Wallingford's Company Research Project DDY0409. This was an extension of the method of Manning and Dyer (2007), using the same extensive data-set gathered in three European estuaries using the in-situ imaging system INSSEV (Fenessy *et al.,* 1994). A similar set of assumptions and interpretations of the data were made in the Company Research Project to those of Manning and Dyer (2007), but whereas their formulation was a purely empirical curve-fit to the data-set, the work in Project DDY0409 introduced a stronger element of basic physics in order to strengthen the assumptions and widen the range of applicability. The resulting formulae and their derivation and testing were presented in HR Wallingford Technical Note DDY0409-01, which is reproduced as Appendix A of the present report. This method is not specifically designed to include the effect of hindered settling, although this can be included separately (together with the effect of turbulence damping due to a vertical density gradient) in computational models.

3.4 IMPLEMENTATION OF SETTLING FORMULATION IN GRIDDED MODELS

The formulations of floc settling velocity and mass settling flux described in Appendix A can be implemented at every vertical level in a vertically gridded model of the flows and sediments in a muddy estuary. This has been tested in a TELEMAC3D model of the Thames estuary. Problems were found in implementing the method very near the bed, where the settling velocity tends to the minimum value $w_{s,av}$ = 0.2 mm/s as the bed is approached. This behaviour can also be seen in Fig. 10 of Appendix A, and occurs because the Kolmogorov microscale (and hence floc diameter) tends to zero as z tends to zero. In practice, the depositional flux of mud is computed at the centre of the lowest cell of the gridded model, so that the minimum value of $w_{s,av}$ is not reached. Nevertheless, the flux is dependent on the vertical grid spacing, which may itself be variable in a model employing sigma-coordinates in the vertical. This is clearly undesirable, but there are many other physical processes that are heavily parameterised and calibrated in such models (e.g. handling of erosion rate from a consolidated bed, inclusion of a depositional unconsolidated layer near the bed, thickness and consolidation and erosion rates of such a layer, downslope flows of dense muddy layers, specification of bed roughness at different spatial scales, smooth versus rough turbulent flows, level at which bed shear-stresses are calculated, specification of bed roughness, etc.). Since none of these processes can be formulated in an unambiguous *a priori* fashion, there is still a strong element of calibration or tuning of the model required, and uncertainties associated with the settling velocity formulation become absorbed into the overall tuning procedure. Until such time as all these processes can be specified more tightly, in an internally consistent manner, tuning of models to observations will continue to be required.

4 Concentration profiles

This section elaborates the derivation of formulae for the vertical profile of suspended mud concentration given in Section 5.4 of DEM.

4.1 OBSERVATIONS

Field observations of vertical profiles of the concentration of suspended mud are commonly made using instruments that measure the attenuation of a beam of light (or sometimes infrared), known as turbidity meters or beam extinction meters. To cope with the high concentrations of mud found in some estuaries, the path-length of the light beam must be short, typically 0.5 cm. A comprehensive survey of mud concentration profiles using this technique was made in the 1970s in a wide range of tidal conditions at 173 profiling stations within the Severn Estuary and inner Bristol Channel, totalling 2193 vertical profiles (Kirby and Parker, 1983; Kirby, 1986). From these, we selected 105 profiles which had concentrations at five or more levels together with current velocity to calibrate and test the diffusional and empirical prediction approaches described below. We developed these approaches as part of a project entitled ‘COAST: Coastal Earth Observation Application for Sediment Transport’ supported by the British National Space Centre, one of whose objectives was to provide predictions of the concentration profile of suspended sediment (for fine sand as well as mud) given a concentration at or near the water surface obtained by remote sensing (Peck *et al*., 1996).

4.2 DIFFUSIONAL APPROACH

The processes determining the variation with height above the bed of the concentration of suspended sediment (the *concentration profile*) are reasonably well understood for non-cohesive sands (Soulsby, 1997). The bed shear-stress due to currents and/or waves acts on individual grains and picks them up from the bed. Vertical water motions due to turbulence carry the sand grains higher into the water column in a diffusion-like process. The grains also experience the force of gravity which, in still water, would carry them downwards with a constant (for a given grain size) settling velocity. A balance between the upward diffusion and the downward settling of grains would give rise to an equilibrium concentration profile, which under constant current and wave conditions can be maintained indefinitely. If the current or wave conditions vary in time or space, the concentration profile of suspended sand adapts reasonably quickly to the new local conditions.

However, the processes for cohesive muds appear to be different. Erosion of the bed takes place continuously if the current or wave flow conditions produce bed shear-stresses greater than the threshold of erosion, τ_e. Thus the concentration of mud in suspension increases until a depth of erosion is reached at which τ_e equals the imposed shear-stress. Only if the shear-stress drops below the threshold of deposition, τ_d (typically about half the value of τ_e) does deposition take place. The settling velocity for suspended mud is a function of the concentration, rather than the grain-size, and hence varies with height. Thus equilibrium profiles for mud do not occur in the way they do for sand. Because settling velocities are generally much smaller for muds than sands, the concentration is more uniform through the water depth. A further consequence is that mud suspensions react much more slowly to changes of the flow in space and time, and therefore mud put into suspension in one part of an estuary is easily carried by the currents to a distant location before it is deposited i.e. the mud transport is dominated by advection, not local processes. Similarly, the temporal reaction of the concentration profile to tidal variations in current, or storm wave events, is much slower, to the extent that the 14-day spring-neap variation in tidal currents can cause greater variations in suspended mud concentration than that within the 12.4 hour tidal cycle.

Despite the above provisos, it is productive to investigate the diffusional approach to determining the concentration profile of mud in a manner analogous to that used for sand, but modified to account for the different behaviour of muds. Such an approach was explored by O'Connor and Tuxford (1980). They tried a variety of different expressions for the variation of diffusivity, settling velocity and erosion/deposition rate, resulting in a number of expressions for the concentration profile, but they did not conclude that any one model gave best predictions.

A simplified diffusional concentration profile for mud suspended by a steady uniform current (without waves) can be derived by making the following assumptions:

a. at every height z the upward diffusive mass flux F_{up} of mud is equal to the downward settling mass flux F_{down} (i.e. the profile is in equilibrium);

b. $F_{up} = -K_s \dfrac{dC_M}{dz}$, where K_s is the eddy diffusivity, and C_M is the dry mass concentration of suspended mud at height z;

c. $F_{down} = w_{50} C_M$, where w_{50} is the median settling velocity of the mud;

d. the eddy diffusivity K_s is constant with height and equated with the eddy *viscosity* observed in the Celtic Sea by Soulsby (1990): $K_s = 0.0025\,\overline{U}h$, where $\overline{U}$ is depth-averaged current speed and h is water depth;

e. for concentrations sufficiently low that hindered settling does not occur, the median settling velocity is given by Equation (5): $w_{50} = kC_M^{\,m}$;

f. the (dry) mass concentration of suspended mud immediately above the bed is C_b.

Starting with $F_{up} = F_{down}$ at all heights, the above equations can be combined to yield an ordinary differential equation:

$$0.0025\overline{U}h\frac{dC_M}{dz} = -kC_M^{m+1} \qquad (12)$$

Equation (12) can be integrated, subject to the boundary condition $C_M = C_b$ at $z = 0$, to give

$$\frac{0.0025\overline{U}h}{-m}\left(C_M^{-m} - C_b^{-m}\right) = -kz \qquad (13)$$

After re-arrangement, Equation (13) yields the diffusional concentration profile:

$$\frac{C_M}{C_b} = \left[1 + B\left(\frac{z}{h}\right)\right]^{-\frac{1}{m}} \quad \text{for } C_b < 3\ \text{kg.m}^{-3} \qquad (14)$$

where $$B = \frac{m\,w_{50b}}{0.0025\overline{U}} \qquad (15)$$

and w_{50b} = median settling velocity immediately above the bed = $kC_b^{\,m}$, i.e. based on Equation (5).

Reasonable agreement has been found between Equation (14) [Equation (5.14) of DEM] and the average of the profiles of suspended mud concentration measured in the Severn Estuary (Figure 3). (Note that individually calibrated values of B were used, rather than Equation 15).

If the mud concentrations are sufficiently large that hindered settling occurs, then Equation (7) should be used in place of Equation (5). However, a simple solution cannot be obtained in this case, and numerical integration is required.

An extended and improved derivation of a diffusional profile, making use of a more sophisticated formulation for settling velocity of flocs than that given by Equation (5), is described in Appendix A. A comparison of the relative performance of Equation (14) and the method described in Appendix A (which requires numerical integration) would be useful if a suitable data-set with all the necessary input information could be found, but this has not yet been done.

4.3 EMPIRICAL APPROACH

The theoretical diffusional concentration profile (Equation 14) decreases smoothly from the bed to the water surface. However, individual measured profiles are extremely variable, sometimes showing smooth profiles, sometimes stepped profiles, sometimes near-bed fluid mud layers. It is likely that no single formula will be able to reproduce such variety of behaviour. Accordingly, a simple alternative is to assume that the concentration decreases linearly with height between the bed and the water surface:

$$C_M(z) = C_b\left(1 - \alpha\frac{z}{h}\right) \qquad (16)$$

where α is a constant <1. If R_c is the ratio of the near-bed concentration, C_b, to the concentration near the water surface, $C_M(h)$, then $R_c^{-1} = 1 - \alpha$. Thus the empirical linearly-varying concentration profile is:

$$\frac{C_M}{C_b} = 1 - \frac{(R_c - 1)}{R_c}\left(\frac{z}{h}\right) \qquad (17)$$

The ratio R_c can either be calibrated against site-specific data if available, otherwise a default value of R_c = 3 can be taken if no data is available. The latter value was found to give agreement to within about a factor of two for 75% of the Severn Estuary data, and gave a similar level of agreement for data-sets at two other sites (with sandy sediments) used in the 'COAST' project data-set.

Extending the comment in the previous sub-section, the performance of Equation (17) could usefully be compared with that of Equation (14) and the profile in Appendix A if suitable data were available.

5 *Conclusions*

Various advances have been made since the first release of this report in 2000. The empirical method for predicting bed shear-stresses on smooth beds described in Section 2 has to a large extent been superseded by the more general method of Soulsby and Clarke (2005). We have given a more detailed description of the method proposed in "Dynamics of Estuarine Muds" for predicting settling velocity of flocculated mud suspensions (Section 3.1), but this is partially superseded by a new method (Section 3.3 and Appendix A) which includes a dependency on the bed shear-stress. However, inclusion of hindering effects in the new method cannot readily be done in the way described in Section 3.1 – it would be too complicated – but hindering can be included as a simple reducing factor based on the volumetric concentration of the flocs. We used the hindered-settling formula to derive better-quantified criteria for the limiting concentration at which hindering significantly affects the settling velocity (Section 3.2). The diffusional (Section 4.2) and empirical (Section 4.3) methods for predicting concentration profiles of suspended mud in quasi-steady, uniform flows have been elaborated on, based on work done in the project 'COAST'.

These improvements have been made to some extent piece-meal, and no attempt has been made here to draw them together as a unified, comprehensive prediction package.

Acknowledgements. In the Company Research reported in Appendix A, I am indebted to Dr Andy Manning for access to his data, and to Drs Manning, Spearman and Whitehouse for substantial inputs into the work. I thank Dr Tom Benson for recounting his experience of implementing the new settling velocity formula in a gridded model.

6 References

Arnskov, M.M., Fredsøe, J. and Sumer, B.M., 1993. Bed shear-stress measurements over a smooth bed in three-dimensional wave-current motion. Coastal Engineering, 20, 277-316.

Burt, T.N. and Stevenson, J.R., 1983. Field settling velocity of Thames mud. Report IT251, HR Wallingford.

Dyer, K. R., 1986. 'Coastal and Estuarine Sediment Dynamics'. John Wiley, Chichester, 342pp.

Fennessy, M.J., Dyer, K.R. and Huntley, D.A., 1994. INSSEV: an instrument to measure the size and settling velocity of flocs in situ. Marine Geology, 117, 107-117.

Fredsøe, J. 1984. Turbulent boudary layer in wave-current motion. J. Hydraulic Engineering, 110, 1103-1120, ASCE.

Grant, W.D. and Madsen, O.S., 1979. Combined wave and current interaction with a rough bottom. J. Geophysical Res., 84(C4), 1797-1808.

Kirby, R., 1986. Suspended fine cohesive sediment in the Severn estuary and inner Bristol Channel, UK. Report ETSU-STP-4042 prepared by Ravensrodd Consultants for UKAEA.

Kirby, R. and Parker, W.R., 1983. Distribution and behaviour of fine sediment in the Severn Estuary and inner Bristol Channel, UK. Canadian J. Fisheries and Aquatic Science, 40 (suppl. 1), 83-95.

Krone, R.B., 1972. A field study of flocculation as a factor in estuarial shoaling processes. Tech. Bulletin 19, Comm. Tidal Hydraulics, US Army Corps of Engineering.

Krone, R. B., 1978. Aggregation of suspended particles in estuaries. In Kjerfve, B. (Ed.), *Estuarine Transport Processes*, Univ. South Carolina Press, 177-190.

Lodahl, C.R., Sumer, B.M. and Fredsøe,J., 1998. Turbulent combined oscillatory flow and current in a pipe. J. Fluid Mechanics, 373, 313-348.

Malarkey, J. and Davies, A.G., 2012. A simple procedure for calculating the mean and maximum bed stress under wave and current conditions for rough turbulent flow based on Soulsby and Clarke's (2005) method. Computers and Geosciences, 43, 101-107.

O'Connor, B.A. and Tuxford, C., 1980. Modelling siltation at dock entrances. Third Symp. Dredging Tecnology, Bordeaux, 359-372, BHRA, Cranfield.

Odd, N.V.M. and Rodger, J.G., 1986. An analysis of the behaviour of fluid mud in estuaries. Report SR84, HR Wallingford.

Peck, T.M., Sweet, R.J.M., Southgate, H.N., Boxall, S., Matthews, A., Nash, R., Aiken, J., Bottrell, H. and Wilson, R., 1996. COAST. Coastal Dynamics '95, Eds. W.R. Dally and R.B. Zeidler, ASCE, pp. 1024-1034.

Puls, W. and Kuehl, H., 1986. Field measurements of the settling velocity of estuarine flocs. Third Int. Symp. River Sedimentation, Jackson, Mississippi, USA.

Sleath, J.F.A., 1990. Velocities and bed friction in combined flows. Proc. 22nd Int. Conf. Coastal Engineering, Delft, 35, 450-463.

Soulsby, R.L., 1990. Tidal-current boundary layers. In: The Sea, Vol. 9A (Ocean Engineering Science), Eds. Le Mehauté, B. and Hanes, D.M., Wiley, New York, pp. 523-566.

Soulsby, R.L., 1995. Bed shear-stresses due to combined waves and currents. In: 'Advances in Coastal Morphodynamics', Eds. M.J.F. Stive, H.J. de Vriend, J. Fredsøe, L. Hamm, R.L. Soulsby, C. Teisson and J.C. Winterwerp, 4-20 to 4-23, Delft Hydraulics, The Netherlands.

Soulsby, R.L., 1997. 'Dynamics of Marine Sands: a Manual for Practical Applications'. Thomas Telford, London.

Soulsby, R.L. and Clarke, S., 2005. Bed shear-stresses under combined waves and currents on smooth and rough beds. Report TR137, R1.0, HR Wallingford.

Soulsby, R.L., Hamm, L., Klopman, G., Myrhaug, D., Simons, R.R. and Thomas, G.P., 1993. Wave-current interactions within and outside the bottom boundary layer. Coastal Engineering, 21, 41-69.

Soulsby, R.L. and Manning, A.J., 2012. Cohesive sediment settling flux: settling velocity of flocculated mud. Tech. Note DDY0409-01 R2.0, HR Wallingford.

Whitehouse, R.J.S., Soulsby, R.L., Roberts, W. and Mitchener, H.J., 2000. 'Dynamics of Estuarine Muds: a Manual for Practical Applications'. Thomas Telford, London.

Figures

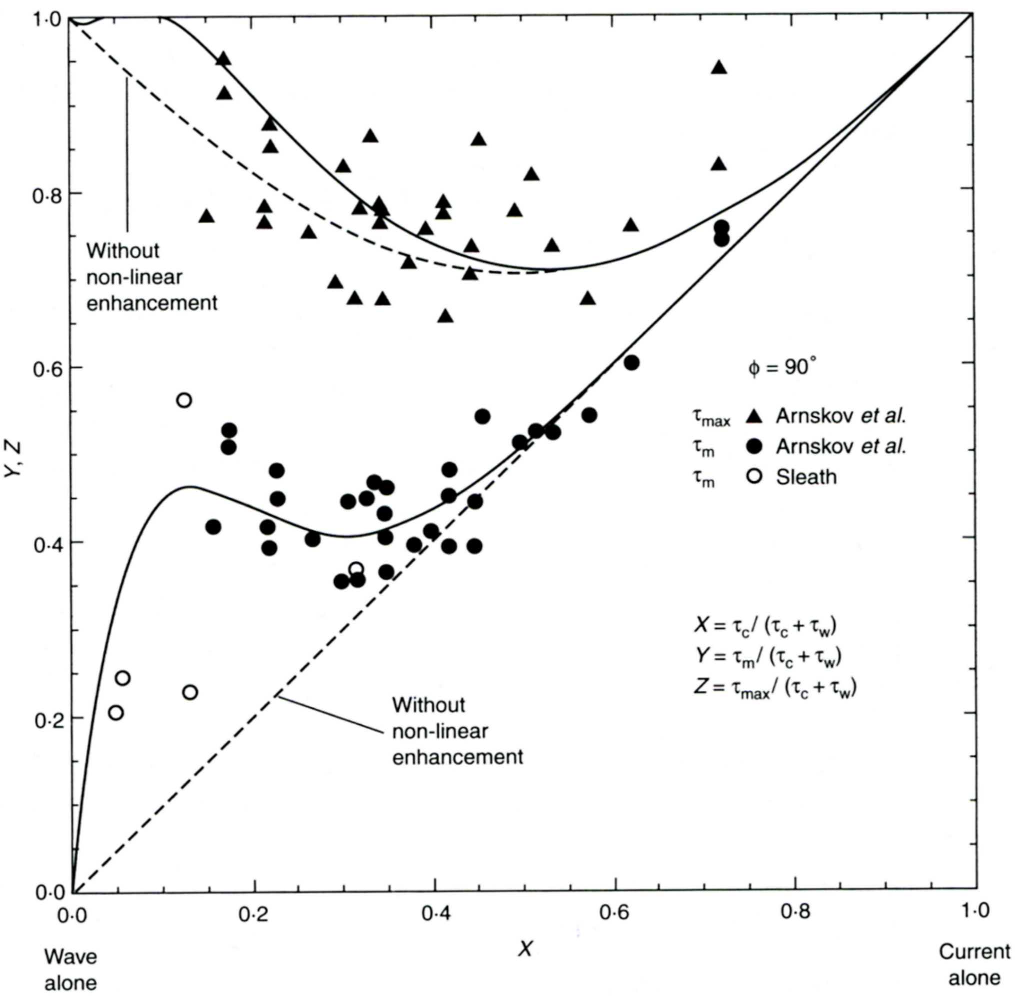

Figure 1 **Comparison of fitted curves with data for the mean τ_m and maximum τ_{max} values of the wave-current shear-stress: waves and currents crossing at right angles. Data from Arnskov et al. (1993) and Sleath (1990). Reproduced with permission from 'Dynamics of Estuarine Muds', published by Thomas Telford Ltd., 2000**

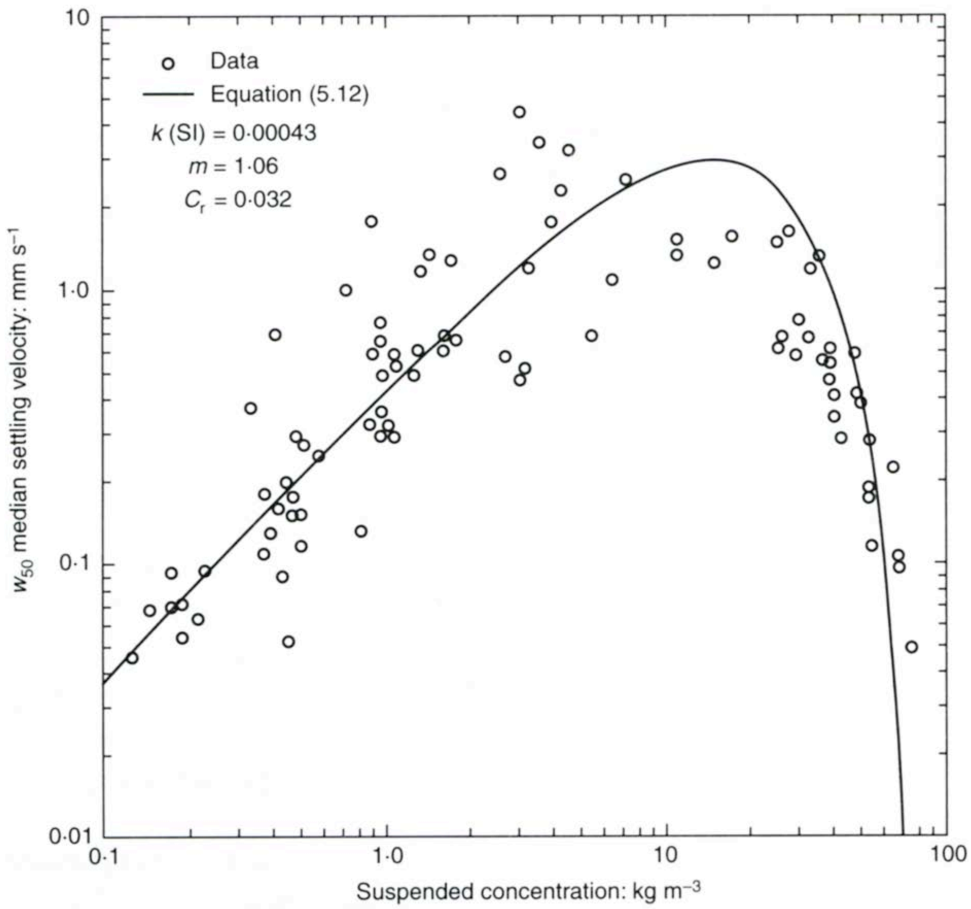

Figure 2 Median settling velocity of Severn Estuary mud as a function of suspended-sediment concentration. Equation (7) plotted for comparison. Owen tube data from Odd and Rodger (1986). Reproduced with permission from 'Dynamics of Estuarine Muds', published by Thomas Telford Ltd., 2000

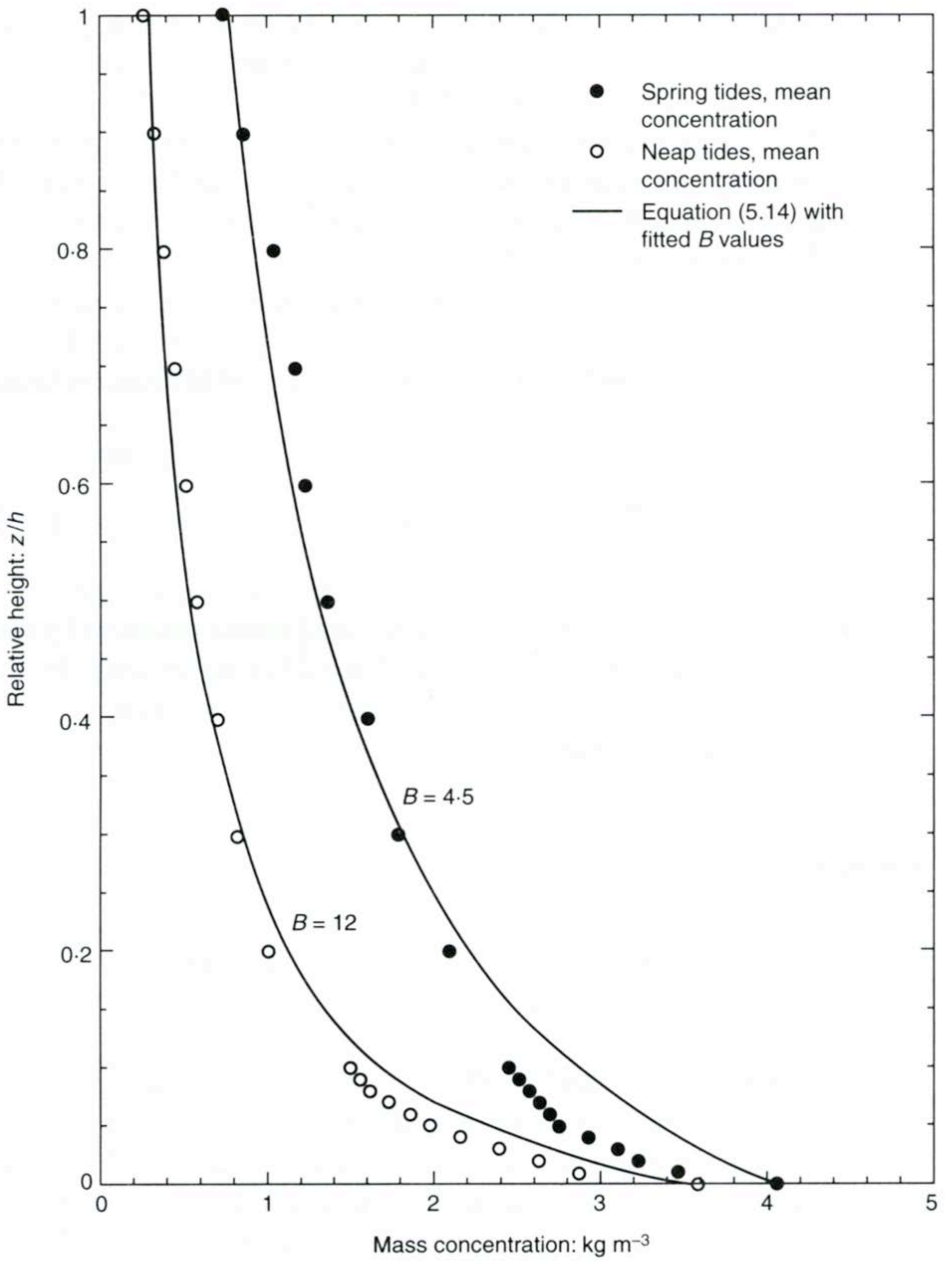

Figure 3 Concentration profiles in Severn Estuary. Comparison of observed mean spring and neap profiles with fitted Equation (14). Data from Kirby (1986). Reproduced with permission from 'Dynamics of Estuarine Muds', published by Thomas Telford Ltd., 2000

Appendix A Cohesive sediment settling flux

Cohesive sediment settling flux

Settling velocity of flocculated mud

R L Soulsby and A J Manning

Technical Note DDY0409-01

HR Wallingford

Address and Registered Office: HR Wallingford Ltd. **Howbery Park, Wallingford, OXON OX10 8BA**
Tel: +44 (0) 1491 835381 Fax: +44 (0) 1491 832233

Document Information

Project	Cohesive sediment settling flux
Technical subject	Settling velocity of flocculated mud
Client	Company Research
Client Representative	Ian Townend
Project No.	DDY0409
Technical Note No.	DDY0409-01
Project Manager	A J Manning
Project Director	R J S Whitehouse

Document History

Date	Release	Prepared	Approved	Authorised	Notes
27/01/12	1.0	RLS	AJM	RJSW	
06/07/12	2.0	RLS	AJM	RJSW	Error in Fig. 10 of R1.0 has been corrected. Descriptive text at end of Section 5 has been altered acccordingly.

Prepared ....

Approved ....

Authorised ....

Acknowledgements

We are indebted to Prof Richard Whitehouse and Dr Jeremy Spearman for constructive comments throughout the project. Tamar Estuary data acquisition was originally part of the EC contract MAS3-CT97-0082 COSINUS (Prediction of cohesive sediment transport and bed dynamics in estuaries and coastal zones with integrated numerical simulation models). The Gironde Estuary data acquisition was funded by the EC TMR SWAMIEE (Sediment and water movement in industrialised estuarine environments) project under contract No. ERBFMRXCT970111. The Dollard Estuary data was acquired during the EC MAST project INTRMUD (The Morphological Development of Intertidal Mudflats) under contract MAS3-CT95-0022.

Summary

New formulations are presented for the settling velocities and mass settling fluxes of flocculated estuarine mud. The mass settling flux is the product of the settling velocity and the sediment concentration, and becomes the depositional flux close to slack water. In this Company Research Project we devised a physics-based set of formulae embodying a similar set of assumptions about the nature of the flocs to those made in earlier work by Manning and Dyer (2007): i.e. a two-class floc population in quasi-equilibrium with the flow, with settling determined only by shear-stress and concentration. We calibrated the formulae against the same large data-set of floc settling imagery that they used (143 in-situ observations of floc size and settling velocity from three estuaries). Whereas the Manning and Dyer formulation was based on multiple regression analysis to fit curves to the data and requires interpolation between piecewise discontinuous equations, the new approach relates floc size and density to the Kolmogorov microscale to give a continuous dependence on both shear-stress and concentration. The number of equations and the number of empirical coefficients are reduced in the new approach. An initial formulation applies only to the near-bed heights sampled by the observations, and the method is then extended to embrace height-dependence and floc-density-dependence. Vertical profiles of concentration, settling velocity and mass settling flux deduced from the new formulae for three example inputs are illustrated. Various measures of performance show that the resulting formulae achieve a similar level of agreement with data to that obtained by the MD07 formulae, while reducing the level of empiricism, and improve on other published prediction methods.

Notation

c dimensionless concentration of sediment (mass of dry sediment/mass of suspension)
c_M dimensionless concentration of Macroflocs (mass/mass)
c_μ dimensionless concentration of microflocs (mass/mass)
d floc diameter (m)
d_1 diameter of primary particles – representative value = 10 μm
d_M diameter of Macroflocs (m)
d_μ diameter of microflocs – representative value = 100 μm
g acceleration due to gravity (taken as 9.81 $m.s^{-2}$)
G velocity shear at microscale = $\upsilon/\eta = (\varepsilon/\nu)^{1/2}$ (s^{-1})
h water depth (m)
MSF mass settling flux of mud ($kg.m^{-2}.s^{-1}$)
r proportion by mass of Macroflocs in SPM = c_M/c
s ratio of densities of sediment mineral and water
s_{eM} ratio of effective density of Macroflocs to that of water
$s_{e\mu}$ ratio of effective density of microflocs to that of water
SPM mass of suspended particulate matter (all sizes) per unit volume of suspension ($kg.m^{-3}$)
TKE turbulent kinetic energy per unit mass of water ($m^2.s^{-2}$)
u_* friction velocity, where $\tau_0 = \rho u_*^2$ ($m.s^{-1}$)
u_{*s} a scaling velocity ($m.s^{-1}$)
w_s settling velocity ($m.s^{-1}$)
$w_{s,av}$ mass-averaged settling velocity ($m.s^{-1}$)
w_{sM} settling velocity of Macroflocs ($m.s^{-1}$)
$w_{s\mu}$ settling velocity of microflocs ($m.s^{-1}$)
z height above bed (m)
z_0 bed roughness length (m)

ε dissipation rate of turbulent kinetic energy per unit mass of water ($m^2.s^{-3}$)
ζ $= z(1 - z/h)$
ζ_f fixed height-scale = 0.5 m
η Kolmogorov microscale (m)
κ von Karman's constant (= 0.40)
ν kinematic viscosity of water taken as 1.03×10^{-6} $m^2.s^{-1}$
ξ $= 1 - z/h$
ρ density of water (taken as 1000 $kg.m^{-3}$)
ρ_e effective density of flocs, including trapped water ($kg.m^{-3}$)
ρ_s density of sediment mineral (taken as 2640 $kg.m^{-3}$)
τ shear-stress in water column ($N.m^{-2}$)
τ_0 bed shear-stress ($N.m^{-2}$)
υ Kolmogorov velocity scale ($m.s^{-1}$)

Subscripts: X_M for Macroflocs, X_μ for microflocs
X_{obs} for observed values, X_{pred} for predicted values
$\overline{X}$ for mean of a set of values of X

Contents

Tables

Contents continued

Figures

1. Introduction

1.1 REMIT

The work described in this report resulted from HR Wallingford Company Research Project DDY0409, whose stated purpose was to develop a "generic physically-based model for the mass settling flux of natural estuarine cohesive sediments". This was achieved by taking as a starting point the empirical formulae for mud floc settling velocity and mass settling flux presented by Manning and Dyer (2007) [referenced in this report as MD07]. The remit was to devise a physics-based set of formulae embodying a similar set of assumptions to MD07 about the nature of the flocs, and calibrate it against the same large data-set of floc settling imagery that they used. Like MD07, the main goal was to achieve a simple yet accurate mathematical description of the vertical mass settling flux (MSF), which becomes the depositional flux close to slack water. This flux is the product of the suspended particulate matter (SPM) concentration and the settling velocity. The aim was to achieve at least a similar level of agreement with data to that obtained by the MD07 formulae, while reducing the level of empiricism.

The MD07 data-set comprised 143 field measurements of the settling velocity and size of mud flocs taken in situ by the INSSEV instrument (Fennessy et al., 1994) in the estuaries of the Tamar (UK), Gironde (France) and Dollard (NL). From these, further analysis by MD07 yielded the effective densities of the flocs through an assumed Stokes Law settling relationship, and the mass settling fluxes of the suspended mud. Details of the three estuaries, the sampling techniques, the instrument and the analysis methods were given by MD07. A further 14 laboratory measurements that were used by MD07 were not included in the present analysis, to ensure that all the measurements used were consistent and natural.

The formulation presented by MD07 made use of the hierarchical division of flocs into microflocs and Macroflocs (e.g. Krone, 1963; Eisma, 1986), elaborated on in Section 2. Note that, because of the similarity in spelling of microflocs and Macroflocs, a capital M will be used for Macroflocs to highlight the distinction. Quantities associated with Macroflocs will be identified by subscript M, and with microflocs by subscript μ.

1.2 BACKGROUND

The remit of the study was set sufficiently wide that all the relevant physical, chemical and biological processes could be considered. At the outset, it was not clear whether including these processes would necessitate a full representation of the detailed mechanisms of floc formation and floc break-up, which might in turn require a time-dependent, multi-fraction approach. Research into the physico-chemical problem of particle aggregation has a long history because of its importance in industrial applications such as chemical manufacturing and waste-water treatment. The book "Particle Deposition and Aggregation" (Elimelich et al, 1995) gives a detailed account of the theoretical and experimental research on this topic. However, because the main industrial interest is in promoting aggregation of particles to enhance settling of solids, only one small section is devoted to floc break-up. In this, the following statements are relevant to determining the size of mud flocs: "the break-up of aggregates is very difficult to model", "Even in laminar shear, it is not easy to predict maximum aggregate size", and "As a convenient rule of thumb, it is sometimes assumed that the limiting floc size in a turbulent flow field is of the same order as the Kolmogoroff microscale". The latter statement will be made use of in the present physics-based approach, and is discussed further below.

Many theoretical treatments of particle aggregation build on the approach developed in a pioneering paper by Smoluchowski (1917), in which the aggregates are divided into a number of size classes. His general approach is neatly summarised by Elimelich et al (1995), and is encapsulated in a differential equation in which the growth rate of the number of aggregates in a given class is related to the gain of new members, and loss of existing members, due to collisions between aggregates in different classes. Four mechanisms giving rise to collisions have been identified (e.g. Dyer, 1986; Krishnappan, 1991; Elimelich et al, 1995; Verney et al, 2010), namely Brownian motion, fluid shear, inertial collision, and differential settling. Expressions for the collision rates of all these mechanisms have been deduced in terms of the sizes of the two classes of aggregate involved in the collision. Expressions have also been proposed for the shear-induced break-up of flocs (e.g. Winterwerp, 1999; Verney et al, 2010), although these are less well-established than those for aggregation. Krishnappan (1991) included all four aggregation mechanisms (but no break-up mechanism) in a model of floc formation and settling in rivers, whereas Winterwerp (1999) and Verney et al (2010) concluded that the most important processes were shear-induced aggregation and shear-induced break-up. Hence low rates of shear increase the size of flocs, high rates of shear reduce the size of flocs, and, for a given shear rate and SPM concentration, an equilibrium distribution of floc sizes will develop after a sufficiently long time. Winterwerp (1999) and Verney et al (2010) developed fully time-evolving, multi-fraction models of floc formation and break-up, which describe the physico-chemical processes in great detail, but in both approaches a number of site-dependent parameters need to be given values, and the models are relatively heavy on computational time.

In practical applications concerning the erosion, transport and deposition of mud in estuaries, various methods of specifying the settling velocity (w_s) of the mud flocs have been used. These methods involve different combinations of input variables, and different numbers of site-specific coefficients to be specified. They are listed in order of increasing complexity below:

1. Specify a fixed value of w_s, usually in the range 0.5-5 mm.s^{-1}, sometimes used as a tuning parameter to match predicted erosion and deposition patterns to observations for the undisturbed estuary. One site-specific coefficient needs to be specified.
2. Relate w_s to the instantaneous SPM concentration through a power law. Two site-specific coefficients need to be specified.
3. Relate w_s to the instantaneous SPM concentration through a power law, including hindered settling (e.g. Whitehouse et al, 2000). Three site-specific coefficients need to be specified.
4. Relate w_s to a turbulent shear parameter and a reference settling velocity (e.g., van Leussen, 1994). Three site-specific coefficients need to be specified.
5. Relate w_s to a turbulent shear parameter and the instantaneous concentration (e.g., MD07). The MD07 method has 27 empirical coefficients derived from their large data-set.
6. Relate w_s to a turbulent shear parameter, instantaneous concentration, and water depth (Winterwerp et al, 2006 Eq 15a). Seven site-specific coefficients need to be specified.
7. Solve a differential equation to deduce the time-varying representative floc diameter, from which floc density is derived by fractal considerations, and w_s

obtained from a Stokes-like formula (Winterwerp, 1999). Six coefficients need to be specified.

8. Apply a time-evolving two-class population balance equation to determine the spatially and temporally changing distribution of size-fixed microflocs and size-varying Macroflocs for bimodal floc distributions, with a fractal relationship between floc size and mass to derive the distribution of settling velocities (Lee et al, 2011). 17 coefficients need to be specified.
9. Apply a time-evolving, multi-fraction, model to determine the spatially and temporally changing distribution of the numbers of flocs in each size fraction, with a fractal relationship between floc size and mass to derive the distribution of settling velocities (Verney et al, 2010). At least seven coefficients need to be specified.

The first six of these methods are relatively quick and easy to apply in practical models of estuarine mud distributions, whereas the the last three are much less straightforward, and more computationally demanding. For the present purpose, it was decided that the fifth option, as used by MD07, gave a good compromise between representation of physico-chemical processes and computational simplicity, and a similar level of sophistication was adopted here. This decision was influenced by the good results obtained from existing HR Wallingford modelling studies incorporating the MD07 method (e.g. Spearman, 2004).

We therefore adopt the two-class approach made up of small, dense microflocs and large, sparse Macroflocs proposed by MD07. The micro/Macrofloc approach was elaborated in the population-balance equations of Lee et al (2011), who modelled the aggregation and fragmentation processes in detail. However, they felt that further intensive investigation of the aggregation and breakage kinetics would be required before their model was generally applicable. The present study takes a simpler approach to the physics, calibrated against the large MD07 data-set, with the intention that the coefficients obtained will be applicable to a wide range of estuarine situations.

No account is taken of hindered settling in this formulation, so its applicability is restricted to SPM concentrations smaller than about 8 $kg.m^{-3}$. The INSSEV data would not be suitable for testing hindering effects, since they cover only concentrations less than 8.6 $kg.m^{-3}$.

2. Fundamentals

2.1 ASSUMPTIONS

MD07 made certain assumptions based partly on the evidence of their field observations, and partly on established principles of mud properties (e.g. Dyer, 1986, 1989). They are adopted in the present formulation, and can be summarised as follows:

1. Flocs are formed from primary particles comprising clay flakes, silt and sand grains, and organic debris. The primary particles are bound together into aggregates by cohesion due to a combination of electro-chemical and organic "glue" forces.
2. The floc population can be divided into two classes: microflocs (made up of a loose aggregate of primary particles) and Macroflocs (made up of a loose aggregate of microflocs). Each class can be characterised by a single size, and the dividing line between microflocs and Macroflocs was empirically set at a spherical-equivalent diameter of 160 μm.
3. The equilibrium size and settling velocity of microflocs are determined only by the turbulent shear-stress (which controls the fine-scale shear and, in turn, the rates of shear-induced floc aggregation and break-up).
4. The equilibrium size and settling velocity of Macroflocs are determined only by the turbulent shear-stress and the overall concentration of suspended particulate matter (SPM).
5. The relative concentrations of microflocs and Macroflocs are determined only by the SPM concentration.
6. Differences in bond strengths between particles due to variations in mineralogy, estuarine water salinity and biological content can be ignored compared with the effects of turbulent shear-stress and SPM concentration.
7. The timescales on which floc formation and break-up operate are sufficiently small that, in a tidal estuarine flow, the floc population can be treated as being in quasi-equilibrium, with floc formation almost balanced by break-up, so that a fully time-dependent approach is not necessary.

On this basis, MD07 devised a formulation for the mass settling flux comprising seven equations obtained by standard regression analysis applied to the data-set, containing 27 empirical (mostly dimensional) fitting coefficients. The MSF is expressed as a function of only SPM concentration and turbulent shear-stress.

The quasi-equilibrium assumption 7, adopted in the formulations of van Leussen (1994), Winterwerp et al. (2006), MD07 and the present approach, permits a considerable simplification of the formulation of w_s and MSF. It ignores the time lag between a change in the flow speed and the response of the floc size and structure: e.g., Verney et al. (2010) showed in laboratory tidal simulations that the floc response could exhibit a lag of more than 20 minutes during floc aggregation, but was almost instantaneous during floc break-up. In most tidal estuary situations assumption 7 is a good approximation, although it might underestimate the initial deposition rate in cases where the flow velocity decreases abruptly (e.g. ingress of turbulent sediment-laden water into a quiescent harbour) and overestimate it where the velocity increases abruptly (e.g. under a tidal bore).

2.2 FLOC PHYSICS

In considering the physics to be included in the new formulation, we again note that the processes involved in aggregation of flocs are well studied, but other processes equally relevant to estuarine mud processes are less well understood (e.g. floc break-up; consolidation and re-erosion of flocs in the settled bed; relative strengths of electro-chemical and biological cohesion; Lagrangian treatment of floc evolution). Hence a detailed analysis of the floc-formation process is not warranted, as the level of complexity would be inconsistent with the treatment of other equally important processes. We therefore adopt the seven assumptions listed in Section 2.1.

Despite considerable differences in opinion concerning many aspects of mud floc behaviour, there is wide agreement that the largest floc sizes are related to the Kolomogorov microscale, η, which is a measure of the finest structure of turbulence (e.g. Van Leussen, 1988; Elimelich et al., 1995; Winterwerp, 1999). Verney et al (2010) found in laboratory tests that the mean floc size was equal to about $\eta/4$ and the maximum floc size (taken as the 90^{th} percentile) was equal to about $\eta/3$. Cuthbertson et al (2010) found in their laboratory tests that the peak floc size (taken as the 95^{th} percentile) was a little larger than $\eta/3$. This connection is elaborated on as follows.

The turbulence properties of flowing fluids follow some well-established and universal relationships (see, for example, Hinze, 1975). In flowing water, turbulent fluctuations in the three components of water velocity are generated at the scales of the largest eddies, which in the case of an estuary are typically constrained by the water depth. The rate of production of turbulent kinetic energy (TKE) is the product of the shear-stress (τ) and the mean velocity gradient ($\partial U/\partial z$). The turbulent eddies break into smaller eddies, carrying the TKE to smaller and smaller scales (the turbulent energy cascade) according to Kolmogorov's '-5/3 law' for the spectral distribution of energy by wave-number within the inertial sub-range of the spectrum (the eddy-scales for which inertia is dominant and viscosity is negligible). At still smaller scales (the dissipation sub-range), the viscosity of the water exerts a significant force through the shear in the small eddies, giving rise to viscous dissipation of the TKE, and a faster decrease in TKE with wave-number. The size of eddy at which viscous forces become important is typified by the Kolmogorov microscale, η. For a steady, uniform flow, the overall dissipation rate (ε) of TKE per unit mass of water is equal to the generation rate by the large eddies. Thus under equilibrium conditions, assuming a logarithmic velocity profile, and neglecting diffusion of TKE:

$$\varepsilon = \frac{\tau}{\rho}\frac{\partial U}{\partial z} = \frac{u_*^3}{\kappa\zeta} \tag{1}$$

where: τ = turbulent shear-stress, ρ = water density, $u_* = (\tau/\rho)^{1/2}$, U is time-mean velocity at height z above the bed, κ is von Karman's constant (taken as 0.40), $\zeta = z/(1-z/h)$, and h is the water depth. For simplicity in Section 3, ζ is set to a fixed value, ζ_f, for all data (even though it is in fact variable), but in Section 4 it is allowed to vary with height.

For eddy-sizes within the dissipation sub-range, Kolmogorov proposed that the turbulence structure depends only on ε and the kinematic viscosity ν of the fluid. He used dimensional reasoning to define a length scale (the Kolmogorov microscale) η and velocity scale υ:

$$\eta = \left(\frac{\nu^3}{\varepsilon}\right)^{1/4} \quad \text{and} \quad \upsilon = (\nu\varepsilon)^{1/4} \tag{2a,b}$$

A characteristic scale for the shear within these small eddies is $G = \upsilon/\eta = (\varepsilon/\nu)^{1/2}$, which is sometimes used to characterise the shear acting on flocs to promote either aggregation or break-up (van Leussen, 1994; Winterwerp et al, 2006; Cuthbertson et al, 2010).

Combining Eqs (1) and (2a) leads to:

$$\eta = \left(\frac{\kappa\nu^3\zeta}{u_*^3}\right)^{1/4} \tag{3}$$

We use similar assumptions to those of MD07 and Winterwerp et al (2006): (a) that the mean diameter of Macroflocs, d_M, is proportional to η, and (b) d_M has a power-law relationship with the (dimensionless) SPM concentration, c. Thus:

$$d_M = \alpha\eta c^k \tag{4}$$

where α and k are dimensionless coefficients. For reasons of dimensional homogeneity, the concentration c is expressed in units of mass of SPM per mass of suspension. Since the settling velocity of Macroflocs, w_{sM}, is very slow (Reynolds numbers $w_{sM}d_M/\nu < 2.2$), the Stokes law of settling is a good approximation:

$$w_{sM} = \frac{(s_{eM} - 1)gd_M^2}{18\nu} \tag{5}$$

in which $s_{eM} = \rho_{eM}/\rho$, ρ_{eM} is the effective density of the Macroflocs and g is the acceleration due to gravity. Similar arguments apply to microflocs.

3. Semi-empirical formula for mud floc settling

3.1 FIXED NEAR-BED HEIGHT

We first derive a formulation that applies only to the height above bed of 0.5-0.6m at which the INSSEV data were collected (corresponding to 6-56 percent of the depth). This is analogous to the approach adopted by MD07 who assumed that floc properties depend only on the *local* τ and SPM, and not explicitly on z. However, this assumption would not be compatible with the link between floc size and Kolmogorov microscale that we make use of here, in which z and h appear independently (see Eqs 1-5). Thus we cannot apply our first approach directly to all heights above the bed, and an extension to a fully height-dependent version is developed in Section 4.

The effective density, ρ_e, of the flocs is relatively small because of the loose nature of the aggregates, with typical values in the range 1.05 to 1.5 kg.m^{-3}. Note that some researchers define effective density of flocs as the excess density relative to water, but here the total density of the water and grains inside a floc is intended.

The effective densities of the flocs observed by the INSSEV instrument were back-calculated for the three estuaries in the data-base. In this section, we assume that the effective specific gravity $s_e = \rho_e/\rho$ is constant for each class of flocs and given by the mean of the 143 observed values: s_{eM} = 1.0708 for Macroflocs, and $s_{e\mu}$ = 1.158 for microflocs. (Seven unrepresentative data-points for the microflocs with $s_{e\mu}$ in the range 1.4 to 2.0 were excluded as they comprised needle-shaped grains of heavy minerals, leaving 136 microfloc data.)

Combining Eqs. (3), (4) and (5) yields:

$$w_{sM} = A(s_{eM} - 1)c^{2k}\left(\frac{g^2\nu\zeta}{u_*^3}\right)^{1/2} \quad (6)$$

where coefficient A combines the dimensionless quantities κ, α and 18. Equation (6) has w_{sM} increasing with c and decreasing continuously with u_*. By contrast, the observations of MD07 (their Figure 2a) show w_{sM} *increasing* with τ for small τ, and reaching a maximum before decreasing with τ (and hence u_*) for large τ . Winterwerp et al (2006) attributed the departure of the data from the behaviour shown by Eq (6) to the limited residence time during which flocs can form, which at small shear-stresses is small compared with the development time of the flocs. Their solution of a differential equation for the rate of growth of (Macro)floc diameter contained a function of ($\tau^{9/8}$ h) which reduced w_{sM} for cases with small shear-stress or depth. A simpler expedient is adopted here, in which Eq (6) is multiplied by an exponential attenuation factor representing this effect. Equation (6) then becomes:

$$w_{sM} = B_M c^m \left(\frac{g^2\nu\zeta}{u_*^3}\right)^{1/2} \exp\left[-\left(\frac{u_{*s}}{u_*}\right)^N\right] \quad (7)$$

where $B_M = A(s_{eM} - 1)$, m = 2k, and B_M, m, u_{*s} and N are optimisable coefficients.

The equation for microflocs is assumed to be of similar form to Eq (7) but with no dependence on concentration. This is based on the similarities between the curves for Macroflocs and microflocs illustrated by MD07 (their Figs 2a,b), but the case is more tenuous because the link between microfloc diameter and η is less well established.

Early tests optimising the coefficients showed that the optimised value of u_{*s} was close to the value for Macroflocs, and the optimised value of N was 1.01. For simplicity, and with little loss of accuracy, the number of coefficients was reduced by setting N = 1 and taking the same value of u_{*s} for microflocs and Macroflocs, resulting in the microfloc equation:

$$w_{s\mu} = B_\mu \left(\frac{g^2\nu\zeta}{u_*^3}\right)^{1/2} \exp\left[-\left(\frac{u_{*s}}{u_*}\right)\right] \quad (8)$$

where $B_\mu = A(s_{e\mu} - 1)$ is an optimisable coefficient.

3.2 CALIBRATION OF COEFFICIENTS

In this section, the scaling height ζ is set to an arbitrary fixed value of ζ_f = 0.5m (the usual measurement height of INSSEV) for *all* data, and this value must always be used when applying Eqs (9) and (10).

Fixed values were taken for calibration purposes of ρ = density of water = 1000kg.m^{-3}, ν = kinematic viscosity of water = $1.03\times10^{-6}\ \text{m}^2.\text{s}^{-1}$, and $g = 9.81\ \text{m.s}^{-2}$. The four coefficients in Eq (7) were optimised against the set of 143 measurements of Macrofloc settling velocity in the MD07 data-base to minimise the sum-of-squared errors, $\sum_{obs}\left(w_{sM\,pred} - w_{sM\,obs}\right)^2$, between the predicted (pred) and observed (obs) w_{sM}. The optimised coefficients are: $B_M = 0.026$, $m = 0.270$, $u_{*s} = 0.025\ \text{m.s}^{-1}$, $N = 0.930$.

A similar optimising procedure for microflocs, Eq (8), using the MD07 data-base for microfloc settling velocity, gave the optimised value $B_\mu = 0.0012$.

Inserting the optimised coefficients, the settling velocities w_{sM}, $w_{s\mu}$ for Macroflocs and microflocs respectively are given by:

$$w_{sM} = 0.026c^{0.27}\left(\frac{g^2\nu\zeta_f}{u_*^3}\right)^{1/2}\exp\left[-\left(\frac{u_{*s}}{u_*}\right)^{0.93}\right] \quad (9)$$

$$w_{s\mu} = 0.0012\left(\frac{g^2\nu\zeta_f}{u_*^3}\right)^{1/2}\exp\left[-\left(\frac{u_{*s}}{u_*}\right)\right] \quad (10)$$

If the inputs are in S.I. units, then w_{sM} and $w_{s\mu}$ are in m.s^{-1}.

The dependence of w_{sM} on τ (Eq 9) is shown (Figure 1a) for a range of values of SPM and compared with the MD07 Macrofloc data, in a similar form to Figure 2a of MD07. The data are colour-coded in bands of SPM, and, if perfectly matched, would lie between the theoretical curve of the same colour and the next curve below it. Although the match is not perfect, partly due to experimental scatter in the data, most of the data-points do lie within or close to the theoretical bands, especially for the larger values of SPM.

A similar comparison for the microflocs (Eq 10 and MD07 microfloc data, Figure 1b) is simpler because there is no dependence on SPM in Eq (10). Again reasonable agreement is found, although there is considerable scatter (though apparently not correlated with SPM) within the range $0.3<\tau<0.7\ \text{N.m}^{-2}$.

The maximum values of w_{sM} and $w_{s\mu}$ occur for a shear-stress of $\tau = 3.9\ \text{N.m}^{-2}$, which is similar to the value of $3.6\ \text{N.m}^{-2}$ in the MD07 formulation. The roll-off of the curves for larger shear-stresses is less steep in Figs 1a,b than in the MD07 formulation. Equations (9) and (10) tend to zero for very small and very large shear-stresses, whereas the MD07 equations tend to constant values which (for w_{sM}) increase with SPM concentration. In practice, a lower limit should be set, corresponding to the settling velocity of the primary particles.

Plots of predicted versus observed settling velocities for Macroflocs (Fig 2a) and microflocs (Fig 2b) show a reasonable clustering around the 1:1 line over a wide range of velocities. The fit for the microflocs is poorer than for the Macroflocs, especially as observed $w_{s\mu}$ in the range 0.7-1.5 mm.s^{-1} are all predicted by values close to 0.8 mm.s^{-1}. This can also be seen in Fig 1b, and in Fig 2b of MD07, and comprises scatter in the data not correlated with shear-stress or concentration. However, such discrepancy is not critical as the overall settling behaviour of mud is often dominated by the Macroflocs.

3.3 MASS SETTLING FLUX

The main requirement for knowing the settling velocity of mud flocs is as an aid to calculating the mass settling flux (MSF). This is the rate at which mud is deposited towards the bed, usually measured in units of $kg.m^{-2}.s^{-1}$, and given by the product of the concentration (as mass per volume) and the settling velocity. In the present two-population model with Macroflocs and microflocs, the MSF is the sum of the individual settling fluxes. This requires division of the total concentration c into concentrations c_M for Macroflocs and c_μ for microflocs, where $c = c_M + c_\mu$. Examination of the data-set of MD07 suggests the following empirical relationship (Figure 3).

Define $X = \log_{10} c + 6$, (numerically equivalent to $\log_{10}(SPM)$ if SPM is in $mg.l^{-1}$). Then the proportion $r = c_M/c$ of the sediment concentration which corresponds to Macroflocs is:

$$r = \begin{cases} 0.1 & \text{for } X < 0 \\ 0.1 + 0.222X & \text{for } 0 \le X < 4.05 \\ 1 & \text{for } X \ge 4.05 \end{cases} \tag{11}$$

Equation (11) gives good agreement between the predicted and observed values of c_M (Figure 4) when compared with the MD07 data-set.

Finally, the total mass settling flux (MSF) is:

$$MSF = [w_{sM}.r + w_{s\mu}.(1 - r)]c\rho \tag{12}$$

Equations (9) to (12) comprise the Soulsby-Manning near-bed (SMN) formulation.

3.4 MEASURES OF PERFORMANCE

To assess the validity of the SMN method, tests have been made that are analogous to those made by Winterwerp et al. (2006) and MD07 of their own methods.

3.4.1 Settling velocity statistics compared with Winterwerp et al. (2006)

Winterwerp et al. (2006) proposed a formula for the settling velocity of Macroflocs, and compared their predictions with observed values for the Tamar (which form part of the total MD07 data-set). They computed measures of goodness-of-fit in two ways: the *absolute* standard deviation (σ_{abs}) between predicted and measured values of (Macrofloc) settling velocity, and the *relative* standard deviation (σ_{rel}) in which the deviation of each data-point is divided by the measured value. They divided the data into classes of concentration range, and also gave values for all the data together. The same procedure has been followed using the SMN method for Macroflocs (Eq 9), but with data from all three estuaries (Tamar, Gironde, Dollard) used. The standard deviations are compared with those of Winterwerp et al (2006) in Table 1.

Table 1 Standard deviations of absolute (σ_{abs}) and relative (σ_{rel}) differences between predicted and measured settling velocities presented by Winterwerp et al (2006), compared with the SMN method (fixed height of 0.5 m above bed).

Conc range kg.m^{-3}	<0.1	0.1-0.2	0.2-0.5	0.5-1.0	1.0-2.0	2.0-4.0	4.0-9.0	All data
Stats for Winterwerp et al (2006) method for Macroflocs in Tamar (their Table 2)								
σ_{abs} mm/s	0.23	0.45	0.72	0.80	1.20	1.11	0.64	0.69
σ_{rel} (%)	17	31	39	35	52	44	15	31
Stats for SMN method for Macroflocs in Tamar, Gironde & Dollard								
σ_{abs} mm/s	0.64	0.51	0.42	0.51	0.61	0.73	0.53	0.58
σ_{rel} (%)	36	24	25	35	26	29	10	31
Stats for SMN method for microflocs in Tamar, Gironde & Dollard								
σ_{abs} mm/s	0.16	0.14	0.21	0.23	0.24	0.15	0.18	0.18
σ_{rel} (%)	32	25	23	18	26	16	17	26

The Macrofloc statistics for the SMN method are better than those of Winterwerp et al (2006) in every concentration range apart from σ_{abs} for SPM < 0.1 and 0.1<SPM<0.2 kg.m^{-3}, and σ_{rel} for SPM < 0.1 kg.m^{-3}. The relative standard deviations lay between 10 and 36 per cent for all the concentration ranges, with the best result for the largest concentrations. The overall absolute deviation was smaller for the new method (0.58 mm.s^{-1} versus 0.69 mm.s^{-1}), and the overall relative deviations were the same for both methods (31 per cent).

A similar analysis (Table 1) using the SMN method for microfloc settling velocities (for which Winterwerp et al did not give a formula), compares predictions using Eq (10) with microfloc data from the three estuaries in the MD07 data-set. The absolute deviations were smaller than for the Macroflocs (as expected, because the settling velocities themselves are smaller), and the relative deviations were in most cases smaller than for the Macroflocs, with an overall relative standard deviation of 26 per cent.

3.4.2 Mass settling flux statistics compared with MD07

MD07 plotted observed versus predicted MSF for their own floc model and four other models (constant w_s = 0.5 and 5.0 mm.s^{-1}, a power-law regression between w_s and SPM, and the method of Van Leussen, 1994) for the 157 cases in their database (including 14 laboratory data). Figure 5 shows a similar plot for the SMN method, but using only the 143 field data, and with the more usual axis convention (predicted versus observed MSF). The fit is good and does not progressively deviate for either small or large MSF. Of the five methods plotted in Figure 3 of MD07 (not shown here), only the MD07 method itself has a comparable accuracy to the SMN method.

MD07 also calculated the cumulative total MSF (i.e. the summation of all 157 individual MSF values) both from their data and from the predictions using the MD07 method and the other four models. Their tabulated statistics are reproduced in Table 2, together with corresponding values from the SMN method. The SMN method compares well with the Manning empirical flocculation method (M1) in all except the standard deviation of the errors. The predicted cumulative total MSF using the SMN method is only 2.3 per cent larger than the observed value, and the mean relative error of the 143 data is less 1 per cent. In almost all the statistics, the SMN method performs better than methods M2 – M5.

Table 2 Summary of statistical tests of accuracy of six methods for predicting MSF
M1: Manning empirical flocculation model; M2: constant w_s = 0.5 mm.s^{-1}; M3: constant w_s = 5.0 mm.s^{-1}; M4: fitted power-law w_{smean} versus SPM; M5: Van Leussen (1994) approach; SMN: Eqs (9-12)

Statistical test	M1	M2	M3	M4	M5	SMN
Mean error (%)	-0.8	-64.5	255.4	-15.4	15.7	-0.98
Std. deviation (%)	10.3	17.9	178.7	34.4	31.8	27.0
Cumul. MSF (pred/obs)	0.964	0.141	1.41	0.651	0.616	1.023
No. of floc samples	157	157	157	157	157	143

4. Extension to vertically-varying version

4.1 ADAPTATION OF APPROACH TO HEIGHT-DEPENDENCY

The SMN formulation derived in Section 3 is directly analogous to that presented by MD07, in that it applies to the INSSEV observations taken at a standard near-bed height of 0.5 m. However, for many purposes it is more valuable to have a formulation for settling velocities and MSF at all heights in the water column. Spearman et al. (2011) extended the MD07 expressions by (a) treating the shear-stresses and concentrations in these expressions as applying at any height, (b) assuming that the shear-stress decreases linearly with height from the bed to the water surface (as in steady uniform flow), (c) including hindered settling via an additional term dependent on the concentration at each height, (d) including density-induced damping of the eddy diffusivity, and (e) computing the concentration profile using an advection-diffusion equation.

The approach given in Section 3 is here extended to include height-dependence so that the observed shear-stress $\tau(z)$ is taken at the true height z in the water column, i.e. not treated as approximately equal to the near-bed shear-stress as was done in Section 3.1. It was further decided to express the settling velocities directly in terms of the dissipation rate, ε, of TKE without making an assumption that the flow is uniform and steady, to allow a more refined approach to be used in flow/sediment models making use of k-ε turbulence closure. A simplified version for the case of steady uniform flow is also presented.

Given the water depth h, the bed shear-stress τ_0 and friction velocity u_* are derived from the observed shear-stress $\tau(z)$ by:

$$\tau_0 = \rho u_*^2 = \tau(z)/\xi \qquad (13)$$

where $\xi = 1 - z/h$. We therefore take $\zeta = z/\xi$ in Eqs (7) and (8); furthermore, the exponential attenuation factor in Eqs (7) and (8) is treated as dependent on $(\tau(z)/\rho)^{1/2} = u_*\xi^{1/2}$ instead of u_*.

4.2 ADAPTATION OF APPROACH TO SIZE-DEPENDENT DENSITY

The excess effective floc density is known to decrease with increasing floc-size (e.g. Elimelich et al., 1995; Winterwerp et al, 2006), and this should be taken into account in the vertically-varying formulation. Elimelich et al. (1995), Winterwerp (1999), Winterwerp et al. (2006) and others assumed that flocs have a fractal nature, in order to establish a power-law relationship between floc density and floc size for a continuum of floc sizes. In the present treatment we do not invoke fractal behaviour of flocs *per se*, but observe that analogous power-law relationships between excess effective density and diameter give reasonably good fits to the MD07 data when separated into the microfloc and Macrofloc populations.

From the full MD07 data-set we exclude the seven anomalously dense microflocs ($\rho_e >$ 1400 kg.m^{-3}) thought to be heavy mineral grains, and two data-points for Macroflocs with anomalously low densities ($\rho_e <$ 1010 kg.m^{-3}) which were thought to contain a high proportion of organic matter. The mean excess effective density of the 136 remaining microfloc data (158 kg.m^{-3}), is considerably larger than that of the 141 Macrofloc data (72 kg.m^{-3}). The corresponding mean effective diameters are 100 μm for microflocs and 255 μm for Macroflocs. The excess effective density is seen to decrease with diameter more steeply for microflocs than for Macroflocs (Figure 6), approximating to power-law relationships. From log-log regressions, these are (in SI units):

$$\rho_{e\mu} - \rho = 1.91\times10^5.d_\mu^{-1.56} \qquad \text{for microflocs} \tag{14}$$

$$\rho_{eM} - \rho = 2.63\times10^3.d_M^{-0.664} \qquad \text{for Macroflocs} \tag{15}$$

Although there is considerable scatter, the R^2 values of 0.371 and 0.147 are both significant at the 99 per cent confidence level. In physical terms, Eqs. (14) and (15) correspond to the mean spacing between particles in a floc increasing with the number of particles constituting the floc. Using this rationale with Eq (14), the density-dependence of microflocs can be re-written in dimensionally homogeneous form as:

$$\frac{s_{e\mu} - 1}{s - 1} = \alpha_\mu \left(\frac{d_\mu}{d_1}\right)^{-1.56} \tag{16}$$

where $s_{e\mu} = \rho_{e\mu}/\rho$, $s = \rho_s/\rho$, ρ_s is the mineral density of the primary particles, d_1 is the (notional) diameter of the primary particles, and α_μ is a dimensionless coefficient. Likewise, taking Macroflocs to be made up of assemblages of microflocs, the density-dependence of Macroflocs (Eq 15) can be re-written as:

$$\frac{s_{eM} - 1}{\bar{s}_{e\mu} - 1} = \alpha_M \left(\frac{d_M}{\bar{d}_\mu}\right)^{-0.664} \tag{17}$$

where $s_{eM} = \rho_{eM}/\rho$, $\bar{s}_{e\mu}$ is the mean relative effective density of microflocs, $\bar{d}_\mu$ is the mean effective diameter of the microflocs, and α_M is a dimensionless coefficient. We take standard values of $s = 2.64$, $d_1 = 10^{-5}$ m (10 μm), $\bar{s}_{e\mu} = 1.15$ and $\bar{d}_\mu = 10^{-4}$ m (100 μm), which should be used in all applications of the method.

4.3 VERTICALLY VARYING SETTLING VELOCITIES

Following the rationale of Section 3, we combine Eqs (7) and (8) with the more realistic height-dependence (Eq 13) and density-dependence (Eqs 16 and 17) to give expressions for the vertically-varying settling velocities. Written in terms of ε, the settling velocities w_{sM}, $w_{s\mu}$ for Macroflocs and microflocs respectively are given by:

$$w_{sM} = B_M(\bar{s}_{e\mu} - 1)\left(\frac{\varepsilon \bar{d}_\mu^4}{\nu^3}\right)^{0.166} gc^{1.336m}\left(\frac{\nu}{\varepsilon}\right)^{1/2} \exp\left[-\left(\frac{u_{*sM}}{u_*\xi^{1/2}}\right)^N\right] \tag{18}$$

$$w_{s\mu} = B_\mu (s-1)\left(\frac{\varepsilon d_1^4}{\nu^3}\right)^{0.39} g\left(\frac{\nu}{\varepsilon}\right)^{1/2} \exp\left[-\left(\frac{u_{*s\mu}}{u_* \xi^{1/2}}\right)^n\right] \quad (19)$$

The coefficients B_M, m, u_{*sM}, N, and B_μ, $u_{*s\mu}$, n, have to be re-calibrated for the height-and-density dependent version. (See note in Section 4.5 for cases with $u_* = 0$ or $\xi = 0$.)

In uniform steady flow, the assumptions of a linearly decreasing shear-stress from bed to water surface and a logarithmic velocity profile lead to the relation:

$$\varepsilon = \frac{u_*^3 \xi}{\kappa z} \quad (20)$$

If ε is not directly available from a flow model with k-ε closure, Eq (20) can be used in Eqs (18) and (19) and is a good approximation in most cases. It is consistent with the underlying assumption that the floc structure is in quasi-equilibrium with the local, instantaneous flow.

4.4 CALIBRATION OF COEFFICIENTS

Not all of the 143 measurements in the MD07 data-base have measured depths, which are required for the height-dependent version. We therefore only used the 113 data with depths (this excludes all the Dollard measurements and some others). The following values of the coefficients in Eqs (18) and (19) were obtained by least-squares optimisation against the reduced data-set, with standard values of s = 2.64, $d_1 = 10^{-5}$ m (10 μm), $\overline{s}_{e\mu} = 1.15$ and $\overline{d}_\mu = 10^{-4}$ m (100 μm). A significantly better fit for microflocs was obtained in this case by retaining the power n in Eq (19) and allowing $u_{*s\mu}$ to take a different value from u_{*sM}. The optimised coefficients are: $B_M = 0.860$, m = 0.165, $u_{*sM} = 0.067$ m.s^{-1}, N = 0.463, $B_\mu = 0.363$, $u_{*s\mu} = 0.025$ m.s^{-1}, n = 0.66.

Comparisons of predicted and observed settling velocities using these coefficients with Eq (18) for Macroflocs (Fig 7a) and Eq (19) for microflocs (Fig 7b) show a similar level of agreement to those for the fixed height formulation (Figs 2a,b).

4.5 MASS SETTLING FLUX

The division between Macrofloc and microfloc contributions to the total SPM was re-calibrated with the same 113 data (differing only slightly from Eq 11):

$$r = \begin{cases} 0.1 & \text{for } X < 0 \\ 0.1 + 0.221X & \text{for } 0 \le X < 4.07 \\ 1 & \text{for } X \ge 4.07 \end{cases} \quad (21)$$

Define the mass-averaged settling velocity $w_{s,av}$ as:

$$w_{s,av} = \max[r.w_{sM} + (1-r).w_{s\mu}\,,\ 0.2\ \text{mm.s}^{-1}] \quad (22)$$

with r(c) given by Eq (21), w_{sM} by Eq (18) and $w_{s\mu}$ by Eq (19). We impose a pragmatic minimum value of $w_{s,av} = 0.2$ mm.s^{-1}, corresponding to the settling velocity of small, tightly-bound microflocs. This value is smaller than any observed values in the MD07 data-base, and hence does not influence the calibration of the coefficients in Eqs (18) and (19). In cases where $u_* = 0$ (slack water) or $\xi = 0$ (sea-bed and water surface), Eqs

(18) and (19) do not apply, and $w_{s,av}$ = 0.2 $mm.s^{-1}$ should be used instead. The mass-averaged settling velocity is similar in concept to the widely-used median settling velocity w_{50} (e.g. Whitehouse et al., 2000) derived from settling columns, but is more directly related to the MSF.

From Eq (12), the total mass settling flux can be written as:

$$MSF = w_{s,av}\, c\rho \qquad (23)$$

Equations (18) to (23) comprise the Soulsby-Manning vertically varying (SMV) formulation.

4.6 MEASURES OF PERFORMANCE

4.6.1 Settling velocity statistics compared with Winterwerp et al. (2006)

The performance statistics for the SMV method, compared with those presented by Winterwerp et al (2006), are shown in Table 2.

Table 3 Standard deviations of absolute (σ_{abs}) and relative (σ_{rel}) differences between predicted and measured settling velocities presented by Winterwerp et al (2006), compared with the SMV method (vertically-varying formulation).

Conc range $kg.m^{-3}$	<0.1	0.1-0.2	0.2-0.5	0.5-1.0	1.0-2.0	2.0-4.0	4.0-9.0	All data
Stats for Winterwerp et al (2006) method for Macroflocs for Tamar (their Table 2)								
σ_{abs} mm/s	0.23	0.45	0.72	0.80	1.20	1.11	0.64	0.69
σ_{rel} (%)	17	31	39	35	52	44	15	31
Stats for SMV method for Macroflocs for Tamar & Gironde								
σ_{abs} mm/s	0.40	0.47	0.43	0.33	0.65	0.68	0.74	0.49
σ_{rel} (%)	27	29	23	12	29	28	14	25
Stats for SMV method for microflocs for Tamar & Gironde								
σ_{abs} mm/s	0.13	0.11	0.18	0.24	0.34	0.18	0.16	0.17
σ_{rel} (%)	25	16	19	20	50	25	15	24

Overall, the figures for the SMV method are an improvement on those in Table 1 for the SMN method, and the Macrofloc statistics for "All data" (0.49, 25%) are better than those of Winterwerp et al (0.69, 31%). All the other Macrofloc statistics are also better than those of Winterwerp apart from σ_{abs} for $c < 0.1$ and $0.1<c<0.2$, and σ_{rel} for $c < 0.1$. The SMV statistics for microflocs (which Winterwerp did not include) are also satisfactorily small.

4.6.2 Mass settling flux statistics compared with MD07

The predicted mass settling fluxes using the SMV method show very good agreement with the MSF measured by MD07 (Fig 8). Of the 113 data from the Tamar and Gironde, 98.2 per cent of the predictions of MSF agree to within a factor of two of the observed values.

A statistical comparison of the performance of the SMV method in predicting the MSF (Table 2) shows a broadly similar performance to that of the SMN method in Table 1. The mean error for the SMV method is slightly larger than for the SMN, but the standard deviation of the errors is slightly improved. The predicted cumulative total

MSF is only 1.3% smaller than the observed value, which is better than any of the other methods.

Table 4 Summary of statistical tests of accuracy of six methods for predicting MSF
M1: Manning empirical flocculation model; M2: constant w_s = 0.5 mm.s^{-1}; M3: constant w_s = 5.0 mm.s^{-1}; M4: fitted power-law w_{smean} versus SPM; M5: Van Leussen (1994) approach; SMV: Eqs (18-23)

Statistical test	M1	M2	M3	M4	M5	SMV
Mean error (%)	-0.8	-64.5	255.4	-15.4	15.7	4.2
Std. deviation (%)	10.3	17.9	178.7	34.4	31.8	26.1
Cumul. MSF (pred/obs)	0.964	0.141	1.41	0.651	0.616	0.987
No. of floc samples	157	157	157	157	157	113

It can be concluded that both the SMV model and the MD07 model give accurate predictions for the (two and three, respectively) estuaries examined. The SMV method also performs better than the other four methods tested, apart from method M2 having a smaller standard deviation.

A further test examines how well the new model predicts the variation of MSF with height z. The MD07 data-set covers the range of heights $0.05<z/h<0.6$. The ratios (predicted MSF)/(observed MSF) plotted for each data-point versus z/h (Figure 9, open symbols) scatter fairly evenly about the line of perfect agreement (pred/obs) = 1. Grouping the data into bands of z/h of width 0.1, the median values in each band (Fig 9, red symbols) cluster tightly about the line (pred/obs) = 1, indicating that the z-dependence of the data is well-represented by Eqs (18-22) for heights up to more than mid-depth. (Median averages are used because the arithmetic mean of a set of ratios is a biassed estimator.)

5. *Vertical profiles in steady uniform flow*

Although the MD07 data-set does not cover elevations much higher than mid-depth, the height-dependence of the new formulae can be tested qualitatively by computing vertical profiles of settling velocity, concentration and mass settling flux. In deriving expressions for the profiles, we assume that the concentrations and their vertical gradients are everywhere sufficiently small that hindered settling effects and turbulence damping of the eddy diffusivity can be neglected. For steady uniform flow, the equilibrium between the mass fluxes of upward diffusion and downward settling of flocculated mud is described by:

$$-\rho K_s \frac{dc}{dz} = \mathrm{MSF} \tag{24}$$

where K_s is the eddy diffusivity of the mud, which we equate with the parabolic eddy *viscosity* profile, thus $K_s = \kappa u_* z(1-z/h)$, consistent with the assumptions made in Section 4 for uniform, steady flow. Making use of Eq (23), this can be written as:

$$\frac{dc}{dz} = \frac{-c w_{s,av}(z, c, u_*, ...)}{\kappa u_* z(1 - z/h)} \tag{25}$$

Equation (25) is an ordinary differential equation that can be integrated numerically over a grid of heights by standard computational methods (e.g. 4th-order Runge-Kutta integration), subject to a boundary condition of a specified concentration at the lowest computational level. This gives the concentration c at each height z, from which the profiles of Macrofloc settling velocity w_{sM} and Macrofloc proportion r can be calculated from Eqs 18 and 21. The microfloc settling velocity profile $w_{s\mu}$ can be calculated from Eq 19, and finally the vertical profiles of $w_{s,av}$ and MSF from Eqs 22 and 23.

Winterwerp (1999, Sec 4.8.1) illustrated profiles from his model of floc settling (without hindered settling) for four cases of steady uniform flow. In each case the water depth was 8m, the bed roughness was z_0 = 1 mm (hydraulically rough) and the depth-averaged concentration of SPM was 1.0 kg.m^{-3}. He considered three depth-averaged current speeds: 0.2, 0.5 and 1.0 m.s^{-1}. We have computed equivalent profiles for the new formulation by integrating Eq (25) using the "ode" numerical integration function in the scientific programming language SciLab, on a uniform grid with 100 points through the water depth, and with reference concentration applied at z = 5 mm. Iteration of the concentration at the bed was used to converge onto the required depth-averaged concentration. Profiles of c, $w_{s,av}$, r and MSF for the three current speeds (Fig. 10) illustrate a number of features (N.B. this replaces text in release R1.0):

a. With this fixed depth-averaged concentration (1.0 kg.m^{-3}), the concentration profiles become more uniformly distributed through the water column as the current speed increases, and have similar shapes and magnitudes to Winterwerp's profiles.
b. The settling velocities lie mainly between 1 and 4 mm.s^{-1} with a mid-water maximum that occurs higher up for stronger flows: the magnitudes are similar to Winterwerp's but the profile shapes are different .
c. A large (50-100 per cent) proportion of the SPM occurs as Macroflocs in these examples (not applicable to Winterwerp method).
d. The shape of the MSF changes markedly with the current speed, being largest near the bed for the low and medium current speeds, but more uniformly distributed for the largest speed (not illustrated by Winterwerp).

6. *Discussion and conclusions*

We have developed new formulations for the settling velocities and mass settling fluxes of flocculated estuarine mud in two stages, by extending the two-class microfloc/Macrofloc empirical model of MD07 through physical reasoning. In the first stage (Eqs 9-12) the method is restricted to the near-bed layer, specifically at the height of 0.5m at which most of the INSSEV measurements were made (SMN method). Coefficients were optimised against the set of 143 measurements of floc size and settling velocity in the Tamar, Dollard and Gironde estuaries presented by MD07. Various measures of performance showed good agreement with the MD07 data-set (Tables 1 and 2, Figs 1-5), lending confidence to the general approach.

In the second stage (SMV method), the derivation was extended by a more rigorous approach to the interpretation of the measured shear-stress, the height-dependence of the Kolmogorov microscale, and power-law relationships between floc effective density and floc size (Figure 6), separately for microflocs (Eq 14) and Macroflocs (Eq 15). The resulting new formulae for the settling velocity of Macroflocs (Eq 18) and microflocs (Eq 19) are written in terms of the dissipation rate of turbulent kinetic energy, ε, making them well-suited for use in computational models of estuaries that employ k-ε turbulence closure. For other types of estuarine model, or for analytical purposes, a quasi-steady assumption is adequate, and ε can be obtained from the relationship for uniform steady flows (Eq 20). The coefficients in the formulae have been optimised using a least-squares technique to the 113 MD07 floc data from the Tamar and Gironde estuaries for which water depth was measured. The resulting coefficients are: $B_M = 0.860$, $m = 0.165$, $u_{*sM} = 0.067$ m.s^{-1}, $N = 0.463$, $B_\mu = 0.363$, $u_{*s\mu} = 0.025$ m.s^{-1}, $n = 0.66$, taken together with standard values of: $s = 2.64$, $d_1 = 10^{-5}$ m, $\overline{s}_{e\mu} = 1.15$ and $\overline{d}_\mu = 10^{-4}$ m.

The division of the total suspended concentration into the proportion r attributable to Macroflocs (Eq 21), and hence the proportion (1-r) attributable to microflocs, leads to expressions for the mass-averaged settling velocity (Eq 22) and the total Mass Settling Flux (Eq 23).

Again various measures of performance have been calculated, and are found to improve on the results found in the first stage. Comparing the predicted Macrofloc settling velocities (Eq 18) with those from the MD07 data-base (Table 3), the absolute r.m.s. deviations are in the range 0.33-0.74 mm.s^{-1}, depending on the concentration, with an overall value of 0.49 mm.s^{-1}. In relative terms, the r.m.s. deviations are 12-29 per cent with an overall figure of 25 per cent. Corresponding statistics for microflocs (Eq 19) give absolute r.m.s. departures of 0.11-0.34 mm.s^{-1} (15-50 per cent in relative terms) dependent on concentration, with an overall value of 0.17 mm.s^{-1} (24 per cent). Apart from data at the lowest concentrations, our Macrofloc statistics show smaller deviations than similar tests reported by Winterwerp et al (2006) for their prediction method tested against data from the Tamar only (their model did not include microflocs).

The predicted values of MSF (Eq 23) compare well with the 113 observed values from the MD07 data-set for the Tamar and Gironde (Figure 8, Table 4). Only one data point lies (just) outside the band of factor-of-two agreement, the mean error is 4.2 per cent and the r.m.s. error is 26 per cent. The predicted integrated MSF (sum of the 113 values) is only 1.3 per cent smaller than the observed value – well within the limits of experimental error. This is even closer to perfect agreement than the method of MD07, although the scatter of individual data about the 1:1 line is greater for the SMV method.

A test of the ability of the SMV method to predict the height-dependence of the MSF (Figure 9) shows that the medians of the ratio (predicted/observed) calculated in bands of width 0.1 in z/h lie within the range 0.94-1.16, and show no consistent deviations from 1.0 within the height range $0.05 < z/h < 0.6$ covered by the data.

A method is described for deriving vertical profiles of all the key quantities by numerical solution of an ordinary differential equation for the concentration (Eq 25) for the case of steady, uniform flow. Plots produced by the SMV method for three hypothetical test cases defined by Winterwerp (1999) are similar in broad terms to the much more elaborate model of Winterwerp: however, no data are available for these examples to compare the model results directly.

The SMV method (Eqs 18-23) looks promising for use in computational models of muddy estuaries. Some comments on applicability are relevant. So far, the method has been calibrated and tested against only two Northern European estuaries, and its generality for use in other situations is not known. If a sufficiently large set of data from other estuaries were available, the coefficients could be re-calibrated either separately for the study case, or combined with the Tamar and Gironde data. In the absence of site-specific data, the coefficients quoted above can be used, with due caution given to the results.

The SMV method has a number of advantages over the already successful method of MD07:

- The inclusion of physical processes in the formulation should, in principle, lead to a broader range of applicability.
- The number of equations has been reduced from seven to five, and the number of empirical coefficients from 27 to 11.
- Equations (18) and (19) cover the entire range of shear-stress, concentration (up to 8 $kg.m^{-3}$), height and depth, which obviates the interpolation procedure required in the MD07 method which caused unrealistic wiggles in their curves (e.g. Fig 2a of MD07).
- The height-dependence of the formulation has been tested against data, from the bed up to mid-depth.
- The level of agreement with data is better than the Winterwerp et al (2006) method (Table 3), comparable with the MD07 method (Table 4), and better than four other methods tested by MD07 (Table 4).
- A simple method of computing vertical profiles of the key quantities for uniform steady flow has been derived (solution of Eq 25 together with Eqs 18 - 23).
- When using the new method in k-ε closure computational models, the non-equilibrium distributions of ε can be input directly in Eqs (18) and (19).
- In such models, the addition of hindered-settling and turbulence-damping processes can be introduced to cover larger concentrations and their gradients than are included in the formulation as it stands (in such cases, both processes should be included, not just one).

7. References

Cuthbertson, A.J.S., Dong, P. and Davies, P.A., 2010. Non-equilibrium flocculation characteristics of fine-grained sediments in grid-generated turbulent flow. Coastal Engineering, Vol. 57(4), pp447-460.

Dyer, K.R., 1986. 'Coastal and Estuarine Sediment Dynamics'. Wiley & Sons, Chichester, UK. ISBN 0 471 90876 2.

Dyer, K.R., 1989. Sediment processes in estuaries: future research requirements. J. Geophys. Res., Vol. 94, No. C10, pp14327-14339.

Eisma, 1986. Flocculation and de-flocculation of suspended matter in estuaries. Neth. J. Sea Res., Vol. 20, No. 2/3, pp183-199.

Elimelich, M., Gregory, J., Jia, X. and Williams, R.A., 1995. 'Particle Deposition and Aggregation: Measurement, Modelling and Simulation'. Butterworth-Heinemann, Woburn, MA. ISBN 0-7506-7024-X.

Fennessy, M.J., Dyer, K.R. and Huntley, D.A., 1994. INSSEV: an instrument to measure the size an settling velocity of flocs in-situ. Marine Geology, Vol. 117, pp107-117.

Hinze, J.O., 1975. 'Turbulence', 2nd edn. McGraw-Hill, NY. ISBN 0-07-029037-7.

Krishnappan, B.G., 1991. Modelling of cohesive sediment transport. Proc. Int. Symp. 'The Transport of Suspended Sediments and its Mathematical Modelling', Florence (Italy).

Krone, R.B., 1963. A study of rheological properties of estuarial sediments. Report No. 63-68, Hyd. Eng. Lab. and Sanitary Eng. Lab., University of California, Berkeley.

Lee, B.J., Toorman, E., Molz, F. and Wang, J., 2011. A two-class population balance equation yielding bimodal flocculation of marine or estuarine sediments. Water Research, Vol. 45, pp2131–2145.

Manning, A.J. and Dyer, K.R., 2007. Mass settling flux of fine sediments in Northern European estuaries: measurements and predictions. Marine Geology, Vol. 245, pp107-122.

Smoluchowski, M., 1917. Versuch einer mathematischen Theorie der Koagulationskinetic kolloider Lösungen. Zeitschrift für Physikalische Chemie, Leipzig, Vol. 92, pp129-168 (in German).

Spearman, J., 2004. Note on the use of algorithms for modelling mud transport on tidal flats. Report TR144 Rev 1.0, HR Wallingford, UK.

Spearman J., Manning A.J. and Whitehouse R.J.S., 2011. The settling dynamics of flocculating mud:sand mixtures: Part 2 - Numerical modelling, Proc. 10th Int. Conf. on Cohesive Sediment Transport, Rio de Janeiro, Brazil, May 2009, Ocean Dynamics, Vol. 61, No. 2-3, pp351-370.

Van Leussen, W., 1988. Aggregation of particles, settling velocity of mud flocs: a review. In: Dronkers, J., van Leussen, W. (Eds.), 'Physical Processes in Estuaries'. Springer-Verlag, Berlin, pp347-403.

Van Leussen, W., 1994. Estuarine macroflocs and their role in fine-grained sediment transport. Ph.D. Thesis, University of Utrecht, The Netherlands, 488pp.

Verney, R., Lafite, R., Brun-Cottan, J.C. and Le Hir, P., 2010. Behaviour of a floc population during a tidal cycle: laboratory experiments and numerical modelling. Continental Shelf Research, Vol. 31(10 supplement), pp. S64-S83.

Whitehouse, R.J.S., Soulsby, R.L., Roberts, W. and Mitchener, H.J., 2000. 'Dynamics of Estuarine Muds'. Thomas Telford, London,UK. ISBN 0 7277 2864 4.

Winterwerp, H., 1999. On the dynamics of high-concentrated mud suspensions. Communications on Hydraulic and Geotechnical Engineering Report No. 99-3, Delft University of Technology, The Netherlands.

Winterwerp, J.C., Manning, A.J., Martens, C., de Mulder, T. and Vanlede, J., 2006. A heuristic formula for turbulence-induced flocculation of cohesive sediment. Estuarine, Coastal and Shelf Science, Vol. 68, pp195-207.

Figures

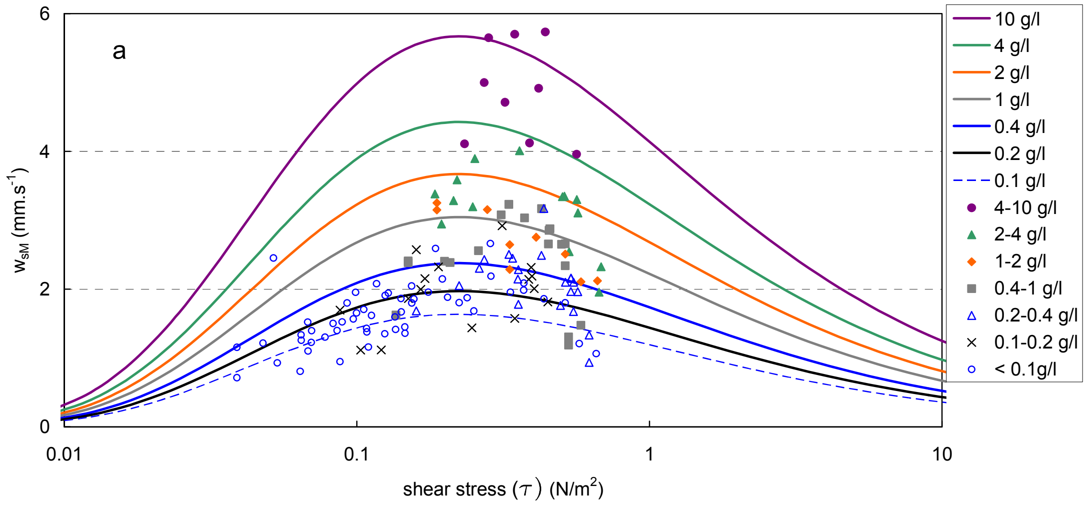

Fig. 1a

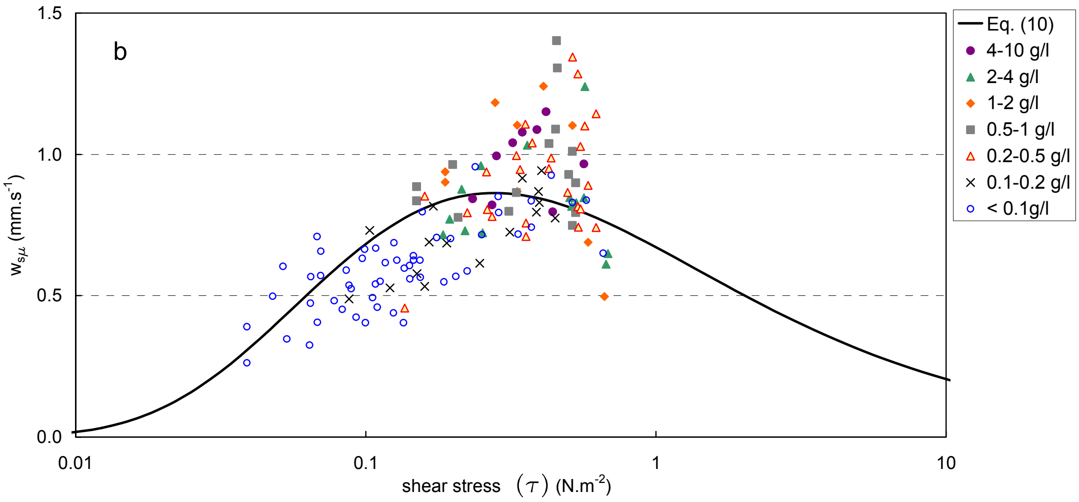

Fig. 1b

Figure 1 **Theoretical curves of settling velocity (SMN method) compared with MD07 data (symbols) for (a) Macroflocs (Eq 9) for selected SPM concentrations 0.1-10 kg.m^{-3} (≡ g/l), (b) microflocs (Eq 10)**

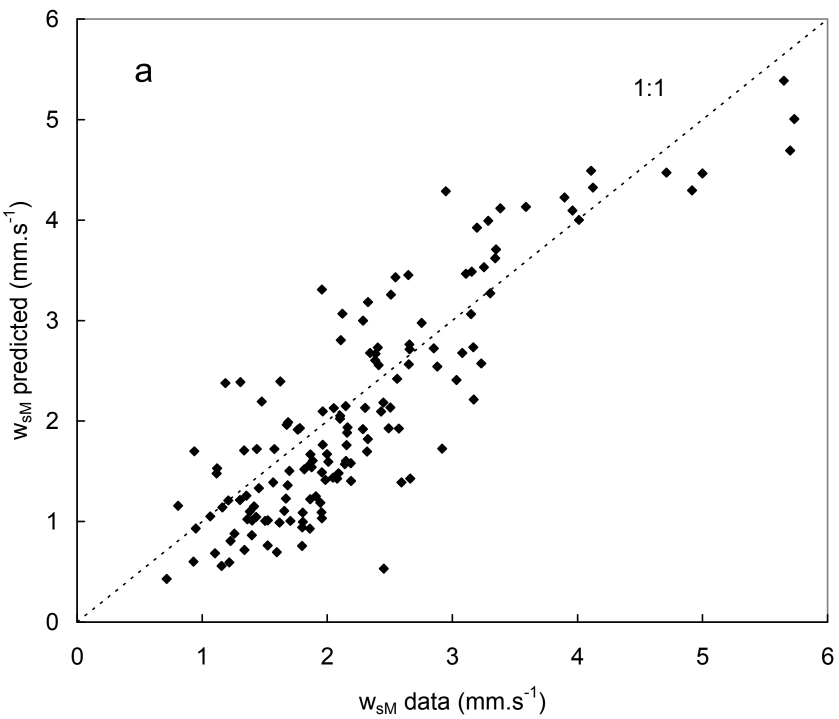

Fig 2a

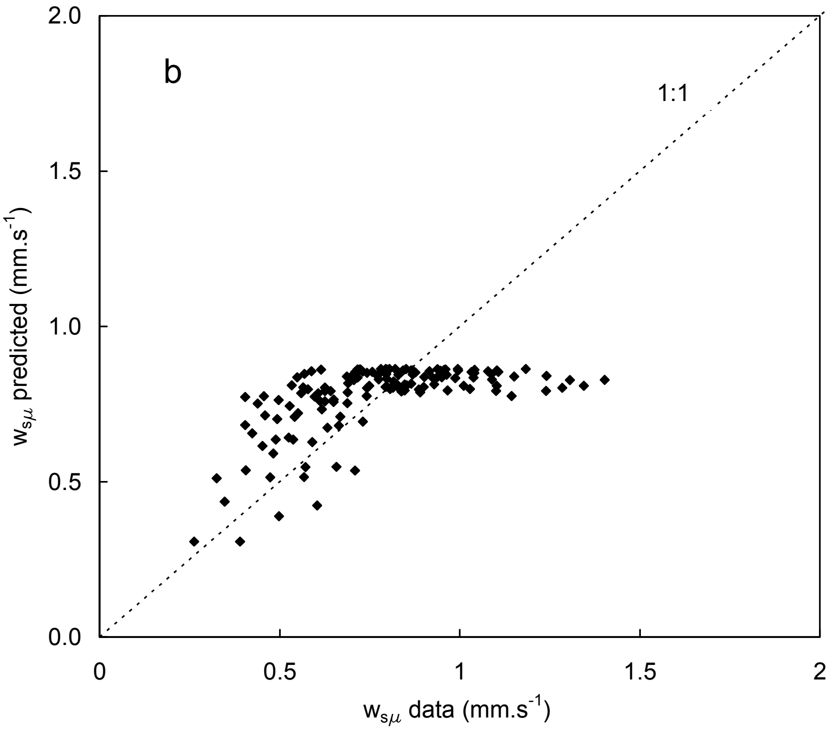

Fig 2b

Figure 2 Comparison of predicted settling velocities (SMN method) with observed values for MD07 data for (a) Macroflocs (Eq 9), (b) microflocs (Eq 10)

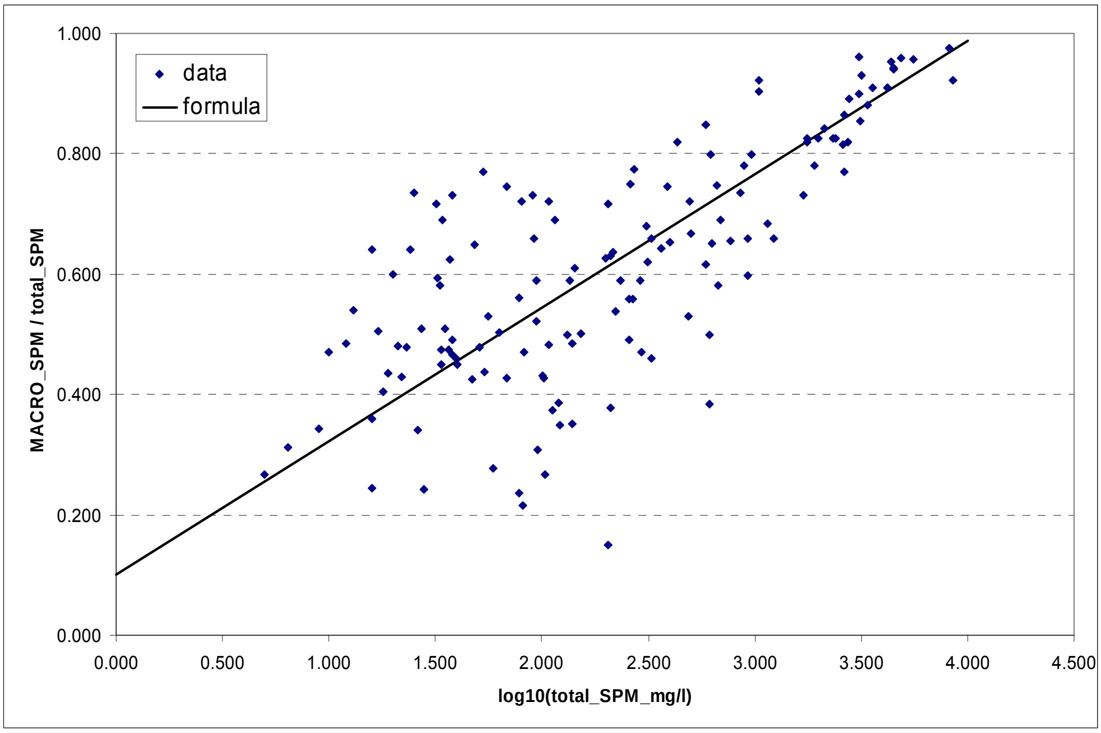

Figure 3 Proportion r of SPM attributable to Macroflocs: MD07 data (symbols) and fitted line (Eq 11) (SMN method)

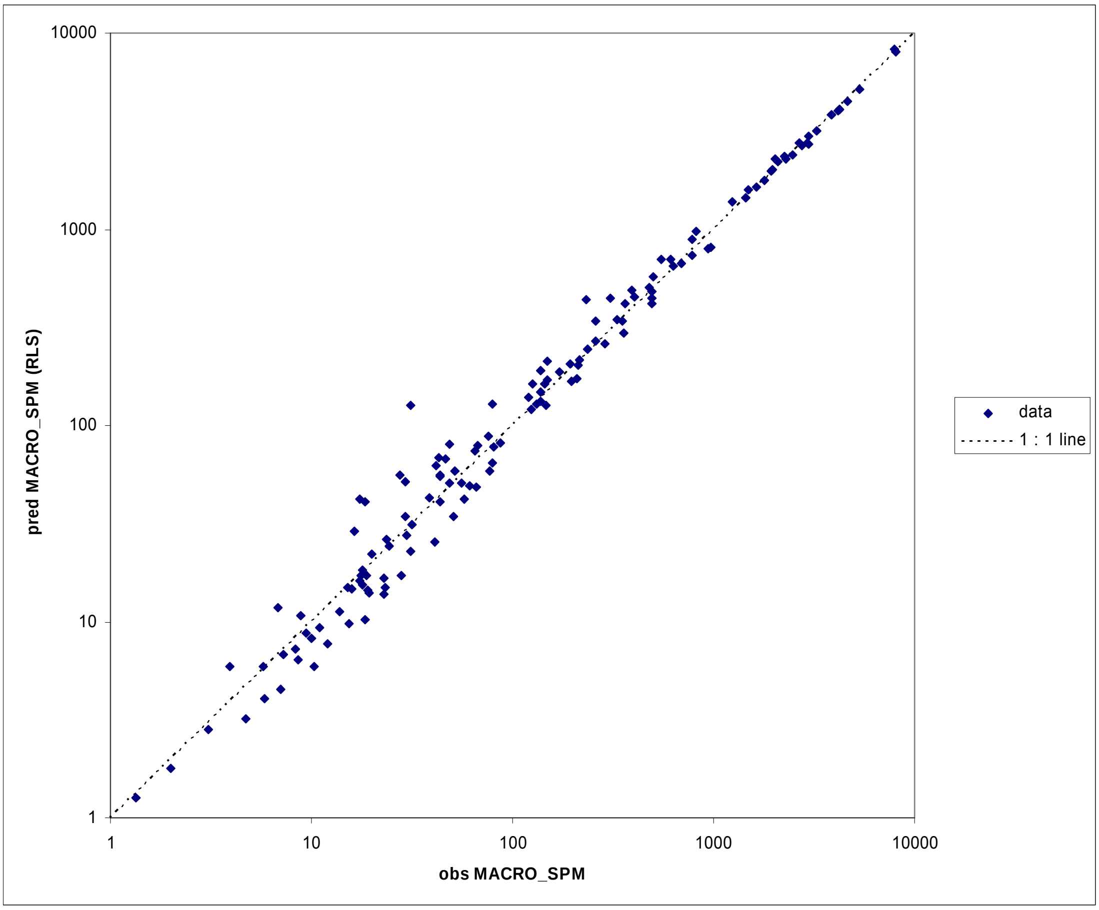

Figure 4 Comparison of predicted (Eq 11) and observed proportion r of SPM attributable to Macroflocs (SMN method)

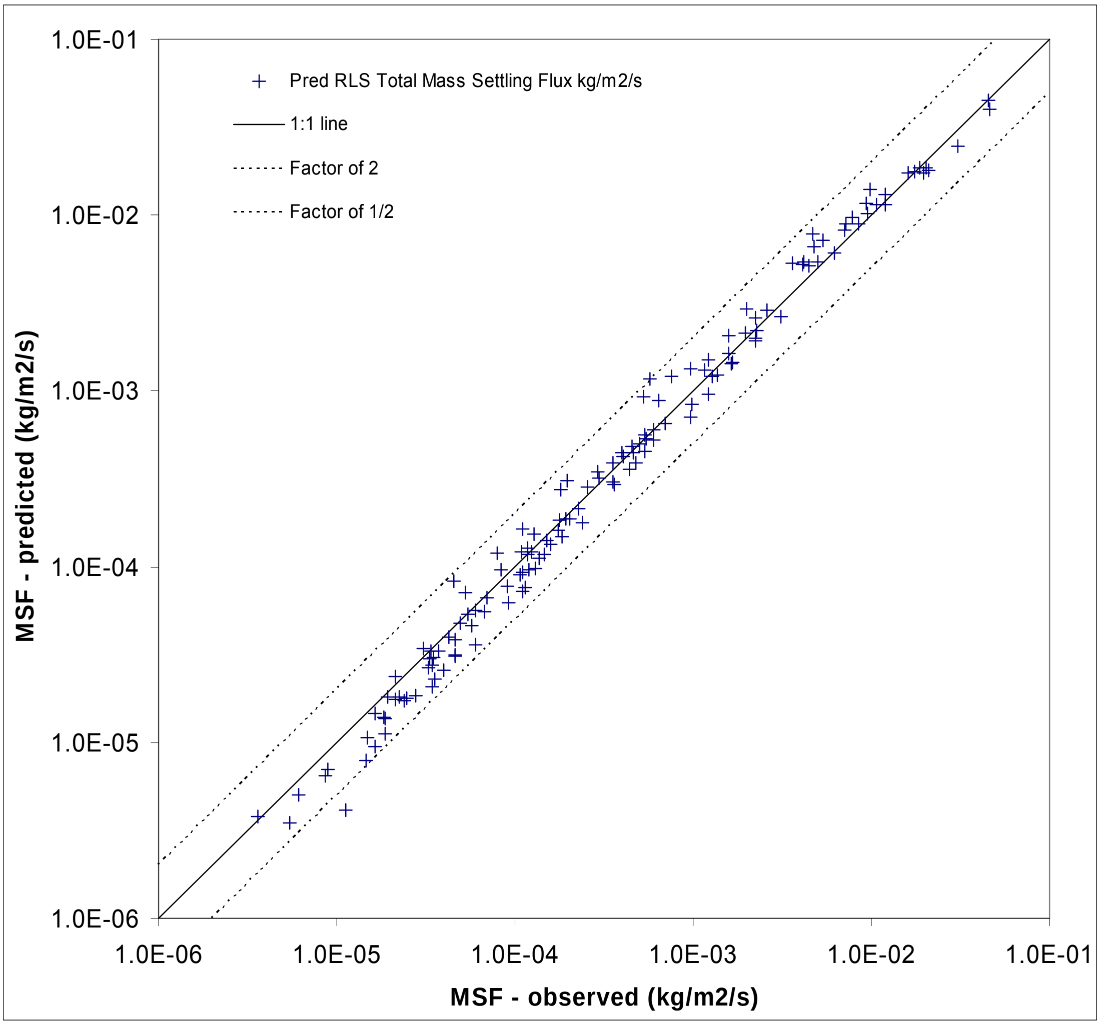

Figure 5 Comparison of predicted (Eq 12) and observed mass settling flux (MSF) for 143 MD07 data for Tamar, Gironde and Dollard (SMN method)

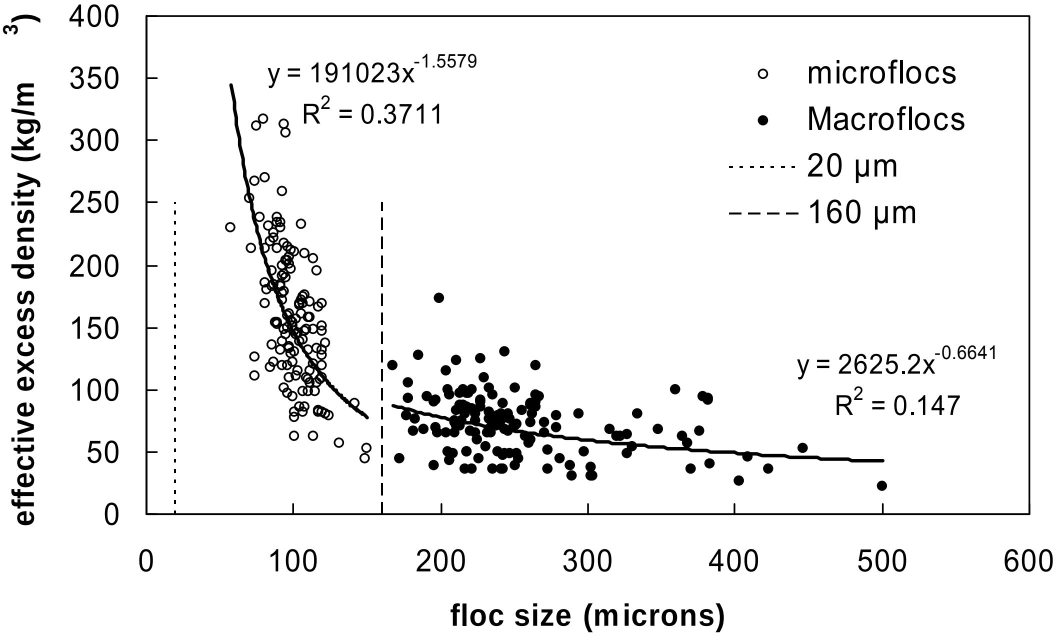

Figure 6 Dependence of effective excess density on floc size with curves fitted separately for microflocs (Eq 14) and Macroflocs (Eq 15)

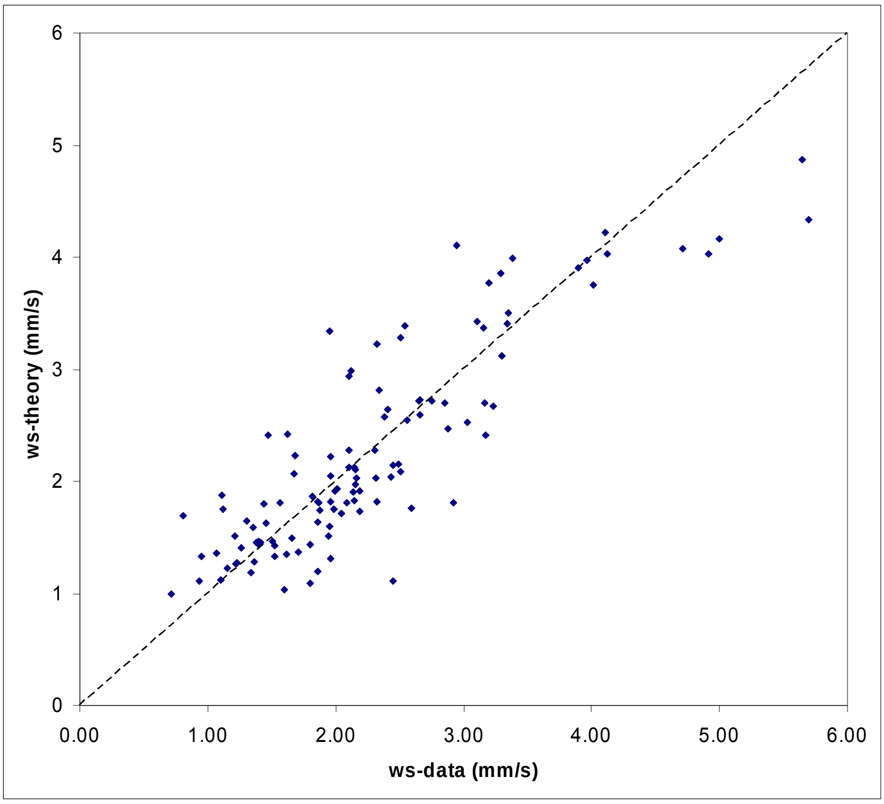

Fig 7a

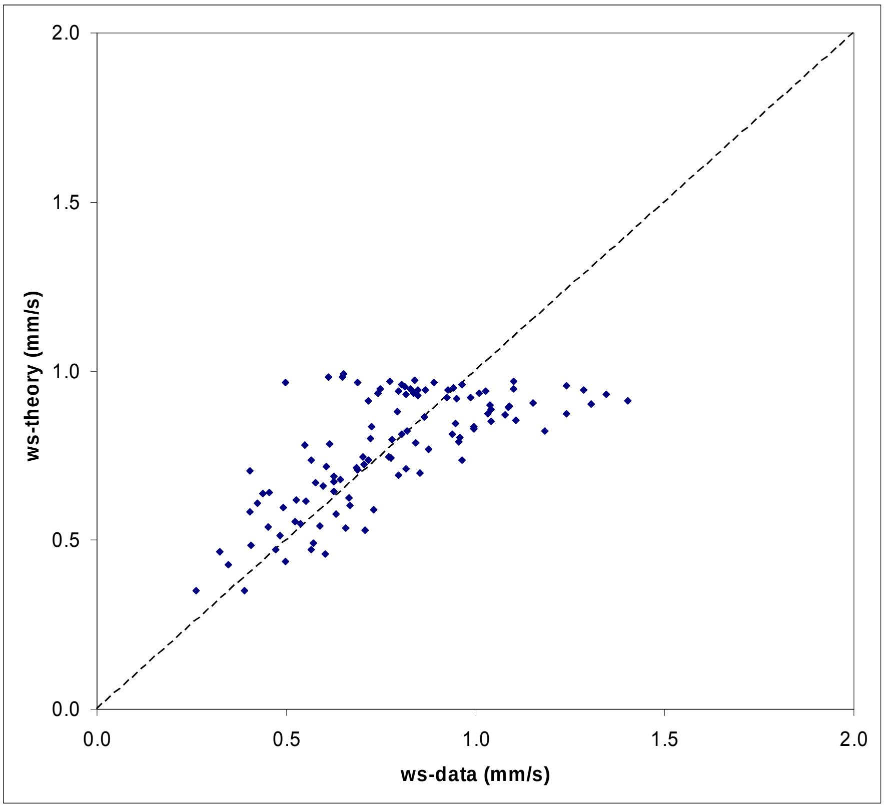

Fig 7b

Figure 7 Comparison of predicted settling velocities (SMV method) with observed values for MD07 data for (a) Macroflocs (Eq 18), (b) microflocs (Eq 19)

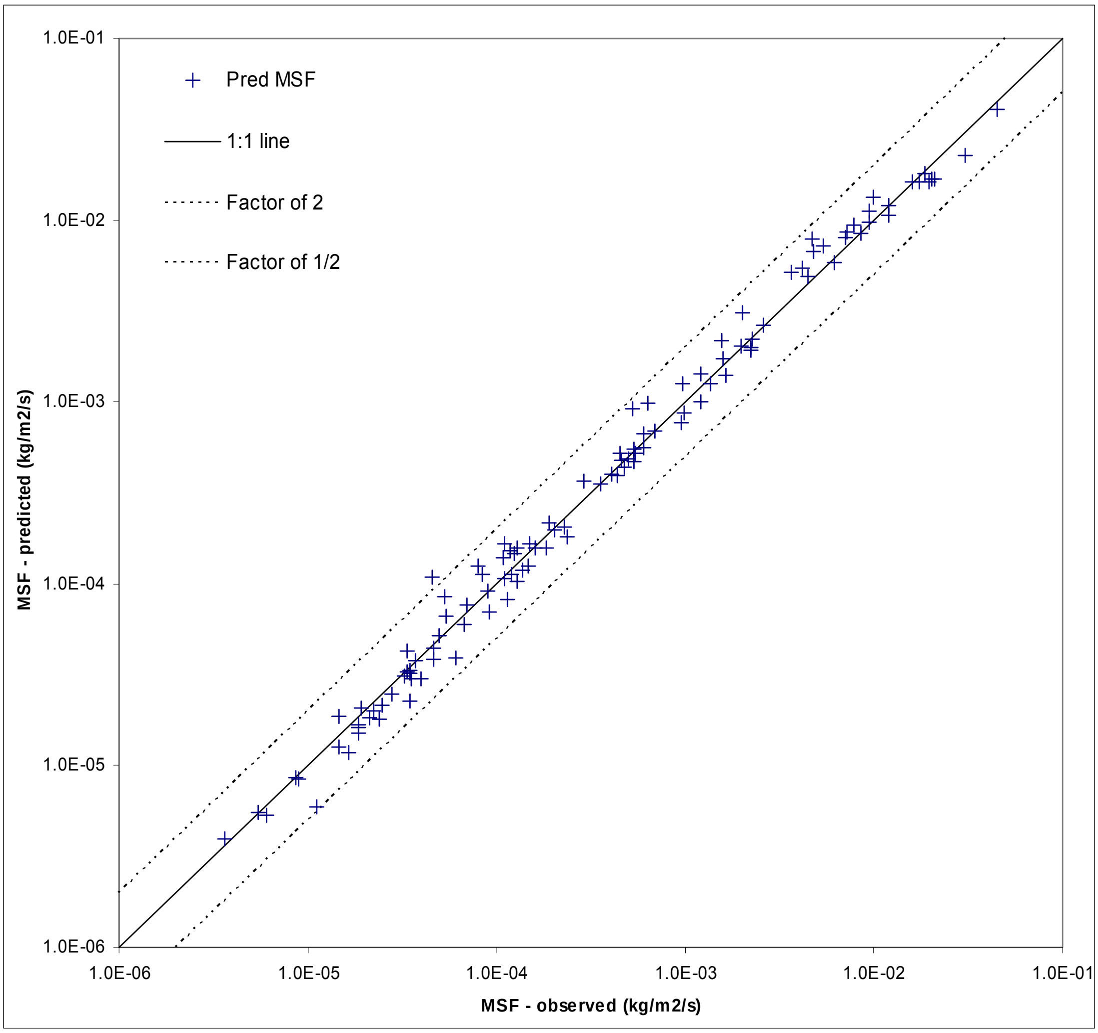

Figure 8 Comparison of predicted (Eq 23) and observed mass settling flux (MSF) for 113 MD07 data for Tamar and Gironde (SMV method)

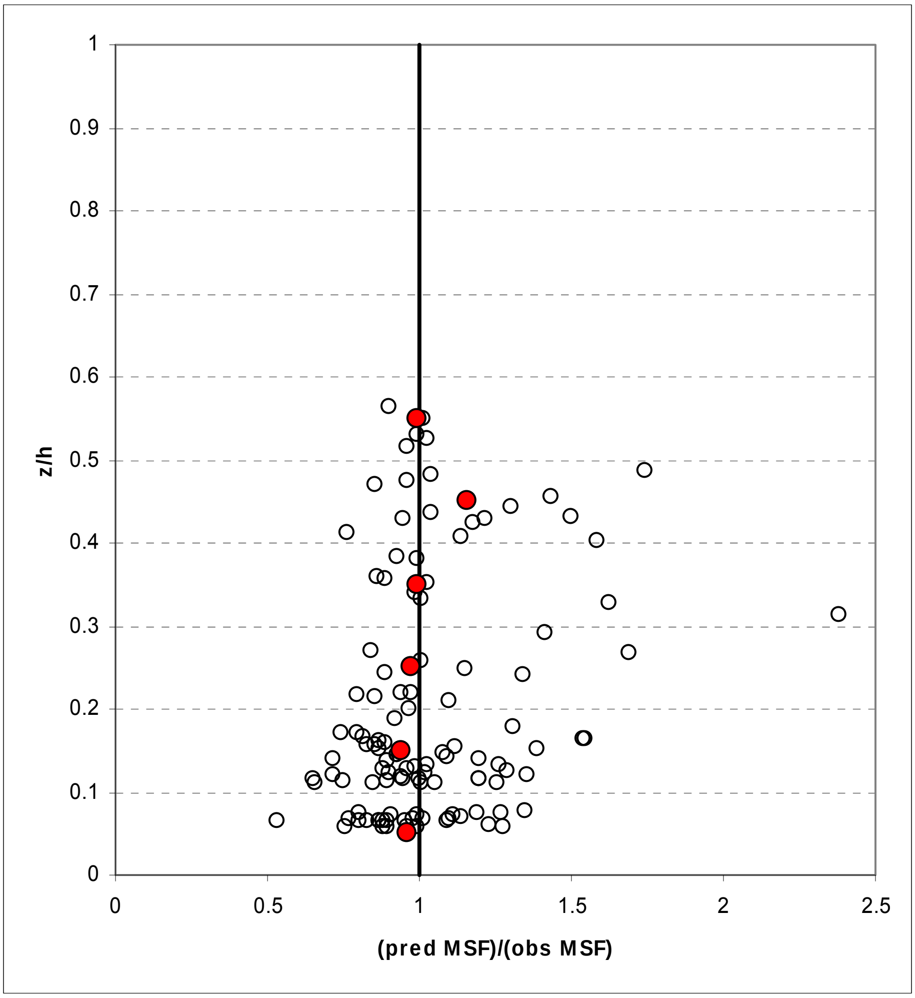

Figure 9 **Test of performance of depth-dependence of predictions of MSF (Eq 23) against 113 observed values in Tamar and Gironde. Open symbols: individual data; red symbols: median values in each band of relative depth z/h of widths 0.1**

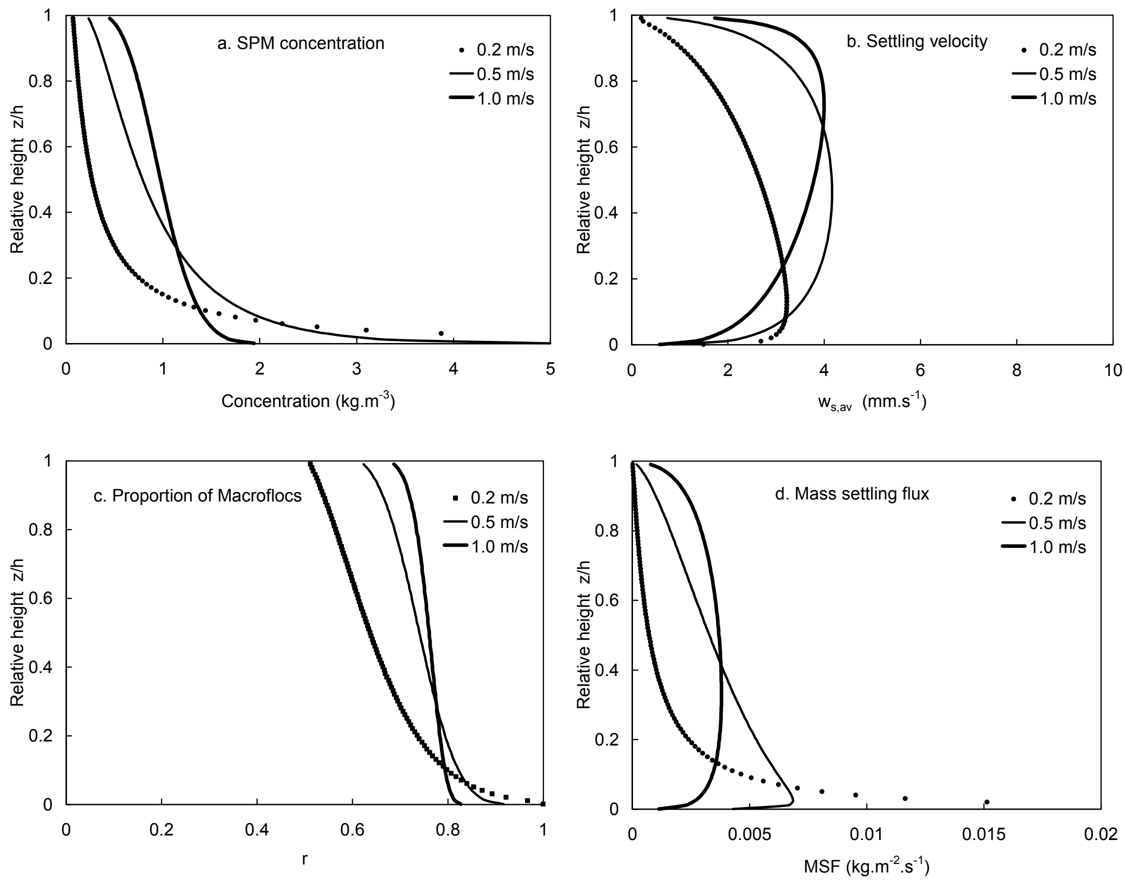

Figure 10 Vertical profiles of c, $w_{s,av}$, r and MSF obtained by numerical integration of Eq (25) for depth = 8m, depth-averaged concentration = 1.0 kg.m^{-3}, z_0 = 1mm and depth-averaged current speeds of 0.2, 0.5 and 1.0 m.s^{-1}

N.B. replaces Figure 10 of release R1.0 which was incorrect

HR Wallingford
Working with water

HR Wallingford is an independent engineering and environmental hydraulics organisation. We deliver practical solutions to the complex water-related challenges faced by our international clients. A dynamic research programme underpins all that we do and keeps us at the leading edge. Our unique mix of know-how, assets and facilities includes state of the art physical modelling laboratories, a full range of numerical modelling tools and, above all, enthusiastic people with world-renowned skills and expertise.

HR Wallingford, Howbery Park, Wallingford, Oxfordshire OX10 8BA, United Kingdom
tel +44 (0)1491 835381 fax +44 (0)1491 832233 email info@hrwallingford.com
www.hrwallingford.com

Certificate No. FS 516431

Certificate No. EMS 558310